### Title

A Combined Experimental and Theoretical Study on the Formation of the 2-Methyl-1-silacycloprop-2-enylidene Molecule via the Crossed Beam Reactions of the Silylidyne Radical (SiH; X(2)Π) with Methylacetylene (CH3CCH; X(1)A1) and D4-Methylacetylene (CD...




### Journal

The Journal of Physical Chemistry A, 120(27)

### ISSN

1089-5639



### Authors

Yang, Tao
Dangi, Beni B
Kaiser, Ralf I
et al.



### Publication Date

2016-07-14

### DOI

10.1021/acs.jpca.5b12457

Peer reviewed

# A Combined Experimental and Theoretical Study on the Formation of the 2-Methyl-1-silacycloprop-2-enylidene Molecule via the Crossed Beam Reactions of the Silylidyne Radical (SiH; $X^2\Pi$) with Methylacetylene ($CH_3CCH$; $X^1A_1$) and D4-Methylacetylene ($CD_3CCD$; $X^1A_1$)

| | |
|---|---|
| Journal: | *The Journal of Physical Chemistry* |
| Manuscript ID | jp-2015-12457n.R1 |
| Manuscript Type: | Special Issue Article |
| Date Submitted by the Author: | 27-Jan-2016 |
| Complete List of Authors: | Yang, Tao; University of Hawaii at Manoa, Chemistry<br>Dangi, Beni; University of Hawaii at Manoa, Chemistry<br>Kaiser, Ralf; University of Hawaii at Manoa<br>Bertels, Luke; University of California at Berkeley, Chemistry<br>Head-Gordon, Martin; University of California, Berkeley, Chemistry |
| | |

# A Combined Experimental and Theoretical Study on the Formation of the 2-Methyl-1-silacycloprop-2-enylidene Molecule via the Crossed Beam Reactions of the Silylidyne Radical (SiH; $X^2\Pi$) with Methylacetylene ($CH_3CCH$; $X^1A_1$) and D4-Methylacetylene ($CD_3CCD$; $X^1A_1$)

Tao Yang, Beni B. Dangi, Ralf I. Kaiser*

*Department of Chemistry, University of Hawai'i at Manoa, Honolulu HI 96822*

Luke W. Bertels, Martin Head-Gordon*

*Department of Chemistry, University of California, Berkeley, Berkeley CA 94720*

Corresponding Authors:

Professor Dr. Ralf I. Kaiser; Email: ralfk@hawaii.edu; Phone: +1-808-956-5731

Professor Martin Head-Gordon; Email: mhg@cchem.berkeley.edu; Phone: +1-510-642-5957

## Abstract

The bimolecular gas phase reactions of the ground state silylidyne radical (SiH; $X^2\Pi$) with methylacetylene ($CH_3CCH$; $X^1A_1$) and D4-methylacetylene ($CD_3CCD$; $X^1A_1$) were explored at collision energies of 30 kJ $mol^{-1}$ under single collision conditions exploiting the crossed molecular beam technique and complemented by electronic structure calculations. These studies reveal that the reactions follow indirect scattering dynamics, have no entrance barriers, and are initiated by the addition of the silylidyne radical to the carbon-carbon triple bond of the methylacetylene molecule either to one carbon atom (C1; [i1]/[i2]) or to both carbon atoms concurrently (C1-C2; [i3]). The collision complexes [i1]/[i2] eventually isomerize via ring-closure to the c-$SiC_3H_5$ doublet radical intermediate [i3], which is identified as the decomposing reaction intermediate. The hydrogen atom is emitted almost perpendicularly to the rotational plane of the fragmenting complex resulting in a sideways scattering dynamics with the reaction being overall exoergic by -12 ± 11 kJ $mol^{-1}$ (experimental) and -1 ± 3 kJ $mol^{-1}$ (computational) to form the cyclic 2-methyl-1-silacycloprop-2-enylidene molecule (c-$SiC_3H_4$; p1). In line with computational data, experiments of silylidyne with D4-methylacetylene ($CD_3CCD$; $X^1A_1$) depict that the hydrogen is emitted solely from the silylidyne moiety, but not from methylacetylene. The dynamics are compared to those of the related D1-silylidyne (SiD; $X^2\Pi$) – acetylene (HCCH; $X^1\sum_g^+$) reaction studied previously in our group, and from there we discovered that methyl group acts primarily as a spectator in the title reaction. The formation of 2-methyl-1-silacycloprop-2-enylidene under single collision conditions via a bimolecular gas phase reaction augments our knowledge of hitherto poorly understood silylidyne (SiH; $X^2\Pi$) radical reactions with small hydrocarbon molecules leading to the synthesis of organosilicon molecules in cold molecular clouds and in carbon-rich circumstellar envelopes.

## 1. Introduction

Over the past few decades, crossed molecular beam experiments have led to an unprecedented advancement in our understanding of fundamental principles of chemical reactivity and reaction dynamics. Detailed experimental studies of three-atom systems such as bimolecular collisions of chlorine (Cl),[1-2] fluorine (F),[3] deuterium (D),[4] carbon (C),[5-6] nitrogen (N),[7-10] oxygen (O),[11-12] and sulfur (S)[13-14] with molecular hydrogen ($H_2$) established experimental benchmarks. The crossed beam approach has been successfully extended to four-atom [OH/CO,[15-17] OH/$H_2$,[16, 18-19] CN/ $H_2$[20]], five-atom [C/$C_2H_2$[21]], and even six-atom systems [Cl/$CH_4$,[22-23] F/$CD_4$[24-26]] bridging our theoretical understanding of reactive scattering dynamics on chemically accurate potential energy surfaces with experimental observations.[27] With the development of powerful theoretical models, attention has turned during the last years to more complex systems of fundamental applications in catalysis, combustion processes, and interstellar chemistry along with planetary atmospheres. This holds in particular for bimolecular reactions between diatomic radicals and small hydrocarbons. Bimolecular reactions involving diatomic radicals such as boron monoxide (BO),[28-35] boron monosulfide (BS),[36-37] methylidyne (CH/CD),[38-45] cyano (CN),[32, 46-60] dicarbon ($C_2$),[57, 61-74] hydroxyl (OH),[75-86] silicon nitride (SiN)[32] and silylidyne (SiH/SiD), [87] synthesized important transient species in extreme environments ranging from low temperature molecular clouds to high temperature combustion settings, interstellar, and chemical vapor deposition environments (Table 1).

Among these diatomic radicals, reactions of the silylidyne radical (SiH; $X^2\Pi$) with hydrocarbons have received particular attention as these bimolecular reactions are expected to result in the formation of small organosilicon molecules ($SiC_xH_y$, $x\leq6$, $y\leq6$). These silicon-carbon-bearing molecules are of essential interest to the astrochemistry community since those species are suggested to comprise nearly 10% of all molecules by mass that have been identified in interstellar and circumstellar environments.[88] However, the underlying reaction pathways, how organosilicon molecules are formed, are unknown to date. Proposed to be a potential key source of refractory material injected into the interstellar medium (ISM),[89] carbon-rich Asymptotic Giant Branch (AGB) stars such as the infrared carbon star IRC+10216 are ideal natural laboratories to test astrochemical reaction networks synthesizing organosilicon molecules in extreme environments (Figure 1).[90,91] Nevertheless, until now, bimolecular ion-molecule

reactions, photochemical processing of circumstellar grains, and reactions on grain surfaces cannot account for the observed fractional abundances of key silicon species such as silicon carbide (SiC) and silicon dicarbide (c-$SiC_2$).[92] These discrepancies are the effect of insufficient laboratory data such as rate constants and reaction products in particular from reactions involving two neutral species.[90, 92-94] Therefore, it is crucial to systematically explore the chemical dynamics of neutral-neutral reactions involving silicon-bearing reaction partners such as the silylidyne radical (SiH; $X^2\Pi$) with hydrocarbon molecules leading to the formation of simple organosilicon molecules ($SiC_xH_y$, $x\leq6$, $y\leq6$) under single collision conditions.[95-98]

These organosilicon molecules have also attracted great interest from the physical organic chemistry community due to the distinct chemical bonding of silicon versus its isovalent carbon counterpart.[99-103] Studies utilizing the crossed molecular beam approach involving isovalent cyano (CN) and silicon nitride (SiN) radicals with acetylene ($C_2H_2$) and ethylene ($C_2H_4$) under single collision conditions revealed the formation of molecules that are distinct in their molecular structures: nitriles (HCCCN, cyanoacetylene; $C_2H_3CN$, vinyl cyanide)[32] and silaisocyano products (HCCNSi, silaisocyanoacetylene; $C_2H_3NSi$, silaisocyanoethylene) [32] (Figure 2). Further, crossed beam reactions of methylidyne (CH) and D1-silylidyne (SiD) with acetylene lead to HCCCH (propargylene)/$H_2CCC$ (vinylidene carbene) and to a minor amount to c-$C_3H_2$ (cyclo-propenylidene) formation [methylidyne reaction],[38] whereas in the D1-silylidyne – acetylene system, the cyclic isomer c-$SiC_2H_2$ (silacyclopropenylidene) was formed exclusively (Figure 2).[87] Therefore, these two case studies document that isoelectronic reactants, in which a carbon atom is replaced by an isovalent silicon atom, can lead to dissimilar reaction products. Consequently, a replacement of a carbon atom by silicon might synthesize novel, hitherto unobserved molecules. Here, we present the results of a crossed molecular beam study on the reactions of the silylidyne radical (SiH; $X^2\Pi$) with methylacetylene ($CH_3CCH$; $X^1A_1$) and with D4-methylacetylene ($CD_3CCD$; $X^1A_1$), respectively, to unravel the reaction mechanism of silylidyne with a prototype C3-hydrocarbon under single collision conditions.

## 2. Experimental Methods

The bimolecular reactions of the silylidyne radical (SiH; $X^2\Pi$) with methylacetylene ($CH_3CCH$; $X^1A_1$) and D4-methylacetylene ($CD_3CCD$; $X^1A_1$) were studied under single collision

conditions in a universal crossed molecular beam machine.[61, 104-108] Briefly, a pulsed supersonic beam of ground state silylidyne radicals (SiH; $X^2\Pi$) was generated exploiting the photolysis of disilane ($Si_2H_6$; 99.998 %; Voltaix) seeded in helium (He; 99.9999 %; Gaspro) with fraction of 0.5 %. This mixture was introduced into a pulsed piezoelectric valve operating at 120 Hz, pulse width of 80 μs, and a backing pressure of 1,520 Torr. The output of an excimer laser (ArF, 193 nm, 30 mJ per pulse) was focused to a spot size of 1 mm × 4 mm and intercepted the molecular beam downstream of the nozzle. The pulsed beam of the silylidyne radicals passed through a skimmer, and a four-slit chopper wheel operating at 120 Hz picked a section of this beam with a well-defined peak velocity ($v_p$) and speed ratio ($S$) of 1730 ± 13 m $s^{-1}$ and 18.9 ± 2.9, respectively. In the interaction region of the scattering chamber, this segment crossed the most intense part of a pulsed (D4-)methylacetylene beam ($C_3H_4$, Organic Technologies; $C_3D_4$, CIL Isotopes) released by a second pulsed valve operating at a backing pressure of 550 Torr perpendicularly. Peak velocities ($v_p$) and speed ratios ($S$) for the methylacetylene and D4-methylacetylene beams were measured to be 800 ± 10 $ms^{-1}$ and 12.0 ± 0.4, and 790 ± 10 $ms^{-1}$ and 12.0 ± 0.4, resulting in nominal collision energies of 30.3 ± 0.7 kJ $mol^{-1}$ and 31.4 ± 1.0 kJ $mol^{-1}$ along with center-of-mass angles of 32.5 ± 0.6° and 34.6 ± 0.6°, respectively. The rotational temperature of the silylidyne radical (SiH; $X^2\Pi$) was determined via laser induced fluorescence (LIF) to be 40 ± 10 K (80 %) and 300 ± 50 K (20 %).[108]

The reactively scattered products were then mass filtered by a quadrupole mass spectrometer (QMS; Extrel QC 150) operated in the time-of-flight (TOF) mode after electron-impact ionization at an electron energy of 80 eV and an emission current of 2 mA. The ions of a well-defined mass-to-charge ($m/z$) ratio were directed toward a stainless steel target coated with a thin aluminum layer floated at -22.5 kV. Triggered by the impact of the cations on the aluminum coated stainless steel target, an electron cascade is generated and accelerated onto an aluminum-coated organic scintillator to initiate a photon pulse, which is further amplified by a photo-multiplier tube (PMT, Burle, Model 8850) operating at -1.35 kV. The signal was filtered by a discriminator (Advanced Research Instruments, Model F-100TD) and fed into a multichannel scaler. At each angle, up to $6\times10^5$ TOF spectra were accumulated. The recorded TOF spectra were then integrated and normalized to extract the product angular distribution in the laboratory frame. The detector is rotatable within the plane defined by both beams to record angular

resolved TOF spectra. To gain information on the scattering dynamics, the laboratory data were transformed into the center-of-mass reference frame using a forward-convolution routine.[109-111] This iterative method exploits a parameterized or point-form angular flux distribution, $T(\theta)$, and translational energy flux distribution, $P(E_T)$, in the center-of-mass (CM) frame. Laboratory TOF spectra and the laboratory angular distributions are extracted from these $T(\theta)$ and $P(E_T)$ functions and averaged over a grid of Newton diagrams accounting for the apparatus functions, beam divergences, and velocity spreads. During the analytical fitting, we considered an integral reactive scattering cross section with an $E_c^{-1/3}$ energy dependence with $E_c$ being the collision energy. This energy dependence is applied for barrier-less reactions dictated by long-range attractive forces within the line-of-center model.[112,113]

## 3. Theoretical Methods

Structures for reactants, products, and intermediates were calculated using density functional theory (DFT) with the ωB97X-V functional[114] and the cc-pVTZ basis set[115] for geometry optimization and frequency analysis (Table S1). Transition-state structures were also computed using the freezing string method (FSM)[116-117] to construct an approximate Hessian followed by a transition-state search using the partitioned-rational function approximation (P-RFO) eigenvector following algorithm[118] and frequency calculation, all also at the ωB97X-V/cc-pVTZ level of theory. The vibrational analysis confirms that the transition states have one imaginary frequency each and the minima have none. The vibrational frequency analysis was also used to compute harmonic zero-point energy corrections for all structures. DFT calculations were carried out using an integration grid consisting of 99 radial points and 590 angular points. All reported energies were computed at the ωB97X-V/cc-pVTZ level, except where otherwise specified. Energies of the reactants, **p1** and **p2** were also computed using coupled cluster with single, double, and perturbative triple excitations [CCSD(T)][119] utilizing a frozen core approximation and second-order Møller-Plesset perturbation theory with the resolution of the identity approximation (RI-MP2).[120-121] To compare directly to experiment, we computed the reaction energies for **p1** and **p2** via

$$(CCSD(T)/CBS) = E(HF/cc-pV5Z) + E^{corr}(RI-MP2/CBS_{4,5}) + E^{corr}(CCSD(T)/cc-pVTZ) - E^{corr}(RI-MP2/cc-pVTZ) + ZPE(\omega B97X-V/cc-pVTZ)$$

where $E^{corr}(RI\text{-}MP2/CBS_{4,5})$ is the extrapolated RI-MP2 correlation energy using the cc-pVQZ and cc-pV5Z basis sets and the extrapolation approach:[122]

$$E^{corr}\left(MP2/(CBS_{M,N})\right) = [N^3 E^{corr}(RI-MP2/cc-pVNZ) - M^3 E^{corr}(RI-MP2/cc-pVMZ)]/[N^3 - M^3]$$

where *M* and *N* denote the cardinal number for the cc-pV*N*Z basis sets. These CCSD(T)/CBS energies are estimated to be converged to within 3 kJ $mol^{-1}$. The coupled cluster results are a higher benchmark that can be used to partially validate the density functional theory used to evaluate the energies of the intermediates. Comparing the ωB97X-V/cc-pVTZ reaction energies with CCSD(T)/CBS reaction energies, we see that the reaction energy for **p1** is changed from -21.4 to -1.0 kJ $mol^{-1}$. This energy change is a measure of the uncertainty in the calculated relative energies of the intermediates. The QChem suite of electronic structure packages was used to perform all calculations.[123]

## 4. Experimental Results

### 4.1. Laboratory Data

For the reaction of the silylidyne radical (SiH; 29 amu) with the methylacetylene molecule ($CH_3CCH$; 40 amu), reactive scattering signal was recorded at *m/z* = 68 ($SiC_3H_4^+$) (Figure 3). Signal at *m/z* = 67 ($SiC_3H_3^+$) was monitored as well, but the corresponding time-of-flight spectra (TOFs) overlapped with those TOFs obtained at *m/z* = 68 ($SiC_3H_4^+$) after scaling. Therefore, signal at *m/z* = 67 stems from dissociative ionization of the parent molecule ($SiC_3H_4$) in the electron impact ionizer. These results indicate that the silylidyne radical versus atomic hydrogen replacement channel forming a molecule with the molecular formula $SiC_3H_4$ is open and that a molecular hydrogen loss channel is closed – at least under our experimental conditions. We would like to highlight that low intensity scattering signal at a level of a few percent of that at *m/z* = 68 was detected at *m/z* = 69. This finding and the fact that the TOFs of *m/z* = 68 and 69 overlap after scaling implies the synthesis of $^{29}SiC_3H_4$ and $^{28}Si^{13}CC_2H_4$; no radiative association at *m/z* = 69 ($SiC_3H_5^+$) occurs in the current system suggesting that the lifetime of the $SiC_3H_5$ adduct is too low to survive the travel from the interaction region to the ionizer. The TOF spectra at *m/z* = 68 ($SiC_3H_4^+$) were then taken at distinct laboratory angles, integrated, and normalized with respect to the center-of-mass reference angle to obtain the laboratory product angular

distribution (Figure 4). This distribution is relatively narrow and spread over only about 25° within the scattering plane as defined by the primary and secondary beam, which indicates a relatively low translational energy release. We also show in Figure 4 the most probable Newton diagram for the reaction of the silylidyne radical (SiH; 29 amu) with the methylacetylene molecule ($C_3H_4$; 40 amu) leading to $SiC_3H_4$ (68 amu) plus atomic hydrogen (1 amu), derived from the assumption that the thermodynamically most stable $SiC_3H_4$ isomer 2-methyl-1-silacycloprop-2-enylidene is formed.[108, 124]

Considering that the hydrogen atom can be emitted from the silylidyne radical or from methylacetylene, we are probing now to what extent the hydrogen atom originates from the hydrocarbon or silylidyne radical. We carried out the crossed beam reaction of the silylidyne radical (SiH; 29 amu) with D4-methylacetylene ($C_3D_4$; 44 amu). An atomic hydrogen loss should yield scattering signal at *m/z* = 72 ($SiC_3D_4^+$), which can fragment to *m/z* = 70 ($SiC_3D_3^+$); on the other hand, an atomic deuterium loss is expected to result in reactive scattering signal at *m/z* = 71 ($SiC_3D_3H^+$). This signal is unique and cannot result from fragmentation of *m/z* = 72 ($SiC_3D_4^+$) formed in a potential atomic hydrogen loss. Considering economic limitations of the costs of the D4-methylacetylene reactant, reactive scattering signal was sampled only at the center-of-mass angle. Here, signal was observed *only* at *m/z* = 72 ($SiC_3D_4^+$) (Figure 5). These data suggest that only the atomic hydrogen elimination pathway is open and that the hydrogen atom likely originnates from the silylidyne radical reactant.

### 4.2. Center-of-Mass Functions

The center-of-mass translational energy distribution $P(E_T)$ is depicted together with the center-of-mass angular distribution $T(\theta)$ in Figure 6. The experimental data could be nicely fit with a single channel utilizing the reactant masses of 29 amu (SiH) plus 40 amu ($C_3H_4$) along with the product masses of 68 amu ($SiC_3H_4$) plus 1 amu (H). In detail, the $P(E_T)$ depicts a maximum translational energy release $E_{max}$ of 45 ± 10 kJ mol$^{-1}$. For products born without internal excitation, this high-energy cutoff represents simply the sum of the collision energy and the absolute value of the reaction exoergicity. A deduction of the collision energy from the maximum translational energy suggests a reaction exoergicity of 15 ± 11 kJ mol$^{-1}$. Further, the $P(E_T)$ peaks at 7 ± 4 kJ mol$^{-1}$. A distribution maximum close to zero translational energy infers

the existence of a loose exit transition state with an inherently small exit barrier to form the $SiC_3H_4$ isomer(s) plus atomic hydrogen.[125] Therefore, considering the concept of microscopic reversibility, we anticipate only a small barrier of hydrogen atom addition in the reversed reaction.[125] Finally, we determined the average fraction of the available energy channeling into the translational degrees of freedom to be 45 ± 9 %.

Further information on the reaction dynamics can be gained by analyzing the center-of-mass angular distribution *T(θ)*. First, the *T(θ)* depicts flux over the complete angular range from 0° to 180° proposing indirect scattering dynamics via complex formation and hence the existence of bound $SiC_3H_5$ intermediate(s)).[125] Secondly, *T(θ)* depicts a distinct maximum at about 90°, suggesting that the atomic hydrogen emission occurs nearly perpendicularly to the rotational plane of the decomposing intermediate(s) and almost parallel to the total angular momentum vector **J**. [113] Finally, the *T(θ)* portrays a mild forward scattering with an intensity ratio *I(0°)/ I(180°)* of about 1.1 : 1.0. This data indicate that the existence of an osculating complex where a complex formation takes place but the well depth along the lifetime of the complex is too low to allow multiple rotations.[126] It should be noted that a forward-backward symmetric distribution results in a slightly worse fit of the experimental data.

## 5. Discussions

We are combining now the experimental data with the results from the electronic structure calculations to elucidate the underlying mechanisms of the reaction of the silylidyne radical (SiH; 29 amu) with the methylacetylene molecule ($C_3H_4$; 40 amu). Let us summarize the experimental results. *First*, the TOF spectra collected at *m/z* = 68 confirm the synthesis of product(s) with the molecular formula $SiC_3H_4$ (68 amu) together with atomic hydrogen (1 amu) under single collision conditions. Additional experiments of the silylidyne radical (SiH; 29 amu) with D4-methylacetylene ($C_3D_4$; 44 amu) provided proof through the explicit detection of $SiC_3D_4$ (72 amu) along with atomic hydrogen that the hydrogen atom is only emitted from the silylidyne moiety, but not from the methylacetylene reactant. *Second*, the formation of the $SiC_3H_4$ isomer(s) plus atomic hydrogen was found to be slightly exoergic by 15 ± 11 kJ mol$^{-1}$; the exit transition state connecting the decomposing $SiC_3H_5$ intermediate and the final products was determined to be loose as reflected in the peaking of the $P(E_T)$ at only 7 ± 4 kJ mol$^{-1}$ suggesting a rather simple Si-

H bond rupture process. *Third,* the center-of-mass angular distribution *T(θ)* proposes indirect scattering dynamics via $SiC_3H_5$ intermediate(s) with lifetime(s) in the order of their rotational period(s). Also, the *T(θ)* was found to peak close to 90º indicating that the hydrogen atom is emitted preferentially parallel to the total angular momentum vector and almost perpendicularly to the rotational plane of the decomposing complex(es).

We are now evaluating the experimentally derived reaction energy and compare the data with the computed energetics to form distinct $SiC_3H_4$ product isomer(s) plus atomic hydrogen. The electronic structure calculations expose that only two $SiC_3H_4$ isomers are energetically accessible at the collision energy of 30 kJ $mol^{-1}$ (Figure 7; Table S1): **p1** and **p2**. It is important to note that our computational investigation identified 28 $SiC_3H_4$ product isomers, whose structures, energetics, and symmetries of the electronic ground states have been disseminated previously.[134] The present analysis places emphasis on those theoretical data crucial to understand the current experimental findings. Here, the synthesis of the 2-methyl-1-silacycloprop-2-enylidene (**p1**) and silacyclobut-2-enylidene (**p2**) isomers was determined to be exoergic (**p1**) and endoergic (**p2**) by -1 ± 3 kJ $mol^{-1}$ and 24 ± 3 kJ $mol^{-1}$, respectively. The experimentally derived reaction energy of -15 ± 11 kJ $mol^{-1}$ slightly falls out of range of the formation of the 2-methyl-1-silacycloprop-2-enylidene isomer (**p1**). However, we have to recall that the LIF characterization of the silylidyne radical beam suggests the silylidyne radicals carry the average rotational temperature of about 3 kJ $mol^{-1}$. A subtraction of the latter from the experimentally derived reaction energy of - 15 ± 11 kJ$mol^{-1}$ – as derived for the condition of no internal excitation of the reactants – reduces the exoergicity of the title reaction to 12 ± 11 kJ $mol^{-1}$; this represents a closer agreement with the computational data of -1 ± 3 kJ $mol^{-1}$. Consequently, **p1** represents the major reaction product. Based on the energetics alone, we cannot eliminate a minor fraction of the thermodynamically less favorable product **p2** at a level of 8 ± 4 %.

Having established that 2-methyl-1-silacycloprop-2-enylidene isomer (**p1**) represents the dominating – if not exclusive – product isomer, we are now developing the underlying reaction dynamics and mechanism(s) by combining the electronic structure calculations with the experimental data. A comparison of the molecular geometries of the silylidyne and methylacetylene reactants with the 2-methyl-1-silacycloprop-2-enylidene and atomic hydrogen

products (**p1**) suggests that the silicon atom is formally added to the carbon-carbon triple bond of the methylacetylene molecule. Therefore, in the reaction of the silylidyne radical with methylacetylene, the silylidyne radical is predicted to add to the carbon-carbon triple bond eventually forming a cyclic $SiC_3H_5$ reaction intermediate (indirect scattering dynamics via complex formation), which then emits a hydrogen atom from the silylidyne moiety. This proposal also gains full support from the reaction of the silylidyne radical with D4-methylacetylene. Here, only an atomic hydrogen atom loss was detected experimentally, but no ejection of a deuterium atom could be monitored, strongly implying that the hydrogen loss originates from the silylidyne moiety, but not from the methylacetylene reactant.

The electronic structure calculations verify these conclusions and expose that the silylidyne radical adds without entrance barrier either to the terminal acetylenic carbon atom (C1) or simultaneously to the terminal and central carbon atom (C1-C2) leading to intermediates [i1]/[i2] or [i3], respectively. These three doublet collision complexes are stabilized by 70, 74, and 174 kJ $mol^{-1}$ with respect to the separated reactants (Figure 7; Table S1); Intermediate [i1] and [i2] are *trans-cis* isomers and are connected via a low lying barrier of only 8 kJ $mol^{-1}$. All attempts to localize an intermediate resulting from the addition of the silylidyne radical to the central carbon atom (C2) failed and resulted in the formation of intermediate [i3]. These initial collision complexes can also isomerize with [i1] and [i2] undergoing ring closure to the much more stable intermediate, [i3], via barriers of only 1 and 8 kJ $mol^{-1}$, respectively. Therefore [i1] and [i2] have only fleeting existence in the dynamics. It is important to highlight that competing hydrogen migrations from [i1] and [i2] to the even more stable intermediate, [i4], are less favorable because of higher barriers to hydrogen migration of 55 and 59 kJ $mol^{-1}$, respectively. Note that intermediates [i4] and [i3] are also connected through the intermediate [i5], which can be formed via cyclization of [i4] followed by hydrogen migration from the silicon to the carbon atom. However, considering the barriers of 1 and 8 kJ $mol^{-1}$ versus 55 to 59 kJ $mol^{-1}$, [i1] and [i2] are expected to readily rearrange to [i3] rather than isomerize to [i4]. This prediction could be also verified experimentally. Here, in the reaction of the silylidyne radical with D4-methylacetylene (Figure 8), addition of the silylidyne radical (SiH) to the carbon-carbon double bond to C1 or C1-C2 leads to [i1'] and [i2'] or [i3'], respectively. From [i3'], hydrogen loss from the Si-H moiety leads solely to D4-2-methyl-1-silacycloprop-2-enylidene isomer (**p1'**). On the other hand,

if a deuterium shift in [i1'] or [i2'] is involved, [i4'] would be formed, too, which isomerizes to [i5']. The latter can undergo either a hydrogen or deuterium shift from the SiHD group forming to distinct intermediates [i3'] and [i3''], which in turn could form **p1'** and **p1''**, respectively, via atomic hydrogen and deuterium loss, respectively. However, since no elimination of a deuterium atom was observed experimentally, we have to conclude that isomers [i4] to [i5] do not play a role in the scattering dynamics, consistent with relative barriers for [i1] and [i2] isomerization as outlined above. Likewise, we can deduce that **p2** is not being formed. Here, **p2** can only be synthesized via the reaction sequence [i3] → [i6] → **p2** + H. However, the barrier for the [i3] → [i6] isomerization of 312 kJ $mol^{-1}$ is too high to compete with the exit barrier-less unimolecular decomposition of [i3] to **p1** plus atomic hydrogen loss.

It is interesting to compare our present studies with the reaction of D1-silylidyne (SiD; $X^2\Pi$) with acetylene ($C_2H_2$; $X^1\sum_g^+$) studied earlier.[87] In both systems, the initial collision complexes were found to be formed barrierlessly by addition of the silylidyne radical to the carbon-carbon triple bond either to one or to both carbon atoms. The initial reaction intermediates reside in relatively shallow (61 to 74 kJ $mol^{-1}$; C1 or C2 addition) and deep (152 to 174 $kJmol^{-1}$; C1 and C2 addition) potential energy wells with the C1/C2 addition products undergoing ring closure via barriers of 1 to 8 $kJmol^{-1}$. The resulting cyclic intermediates fragment via atomic hydrogen loss solely from the SiH moiety via loose exit transition states with the hydrogen atom emitted almost perpendicularly to the rotation plane of the decomposing complex in overall weakly exoergic reactions (-1 to -10 $kJmol^{-1}$). The exclusive formation of the silacyclopropenylidene molecule (c-$Si_2H_2$) in the D1-silylidyne with acetylene system under single collision conditions indicates that in the silylidyne – methylacetylene system, the methyl group acts mainly as a spectator. However, we would like to stress that in the silylidyne – methylacetylene reaction, no addition product of the silylidyne radical to C2 was observed; this suggests that the bulky methyl group and silylidyne moiety 'repel' each other and shift the silylidyne moiety closer to the C1 carbon atom resulting in formation of [i3].

To summarize, the computations suggest that the silylidyne radical can add barrierlessly via three open entrance channels to yield intermediates [i1] to [i3] (Figure 7). This indirect reaction dynamics via complex formation were proposed from the center-of-mass angular

distribution exhibiting intensity over the whole scattering range. Intermediates [i1] and [i2], which are likely formed via trajectories holding large impact parameters via addition of the silylidyne radical to the sterically less hindered carbon atom of the methylacetylene reactant, undergo facile ring closure to [i3] with barriers less than the energy of the separate reactants. Eventually, intermediate [i3] undergoes unimolecular fragmentation via atomic hydrogen elimination from the silylidyne group yielding 2-methyl-1-silacycloprop-2-enylidene isomer (**p1**). The electronic structure calculations suggest a barrierless dissociation while the experimental data imply that this process is connected with a rather loose transition state considering the weakly off-zero peaking of the center-of-mass translational energy distribution at $10 \pm 3$ kJ mol$^{-1}$. In this case, considering the reversed reaction by the addition of a hydrogen atom to the closed-shell and partially aromatic ($2\pi$) molecule **p1**, the likely presence of a small entrance barrier to hydrogen atom addition seems sensible. This addition could also be reflected considering the ejection of the hydrogen atom nearly perpendicularly to the rotational plane of the decomposing complex. For the addition of a hydrogen atom to **p1**, the HOMO and LUMO of the latter would depict a maximum overlap with the 1s orbital of the hydrogen atom if a trajectory nearly perpendicularly to the molecular is followed (Figure 9).

## 6. Summary

We carried out the crossed molecular beam reaction of the ground state silylidyne radical (SiH; $X^2\Pi$) with methylacetylene ($CH_3CCH$; $X^1A_1$) and with D4- methylacetylene ($CD_3CCD$; $X^1A_1$) at collision energies of 30 kJ mol$^{-1}$. Electronic structure calculations indicate that the reaction of silylidyne with methylacetylene has no entrance barrier and is initiated by the silylidyne radical addition to the $\pi$ electron density of the methylacetylene molecule either to the sterically less hindered C1 carbon atom or to the C1-C2 carbon atoms simultaneously. The complexes formed through indirect scattering dynamics were also verified by the center-of-mass angular distribution. The originally formed addition complexes [i1] and [i2] rearrange readily via ring closure to form the cyclic $SiC_3H_5$ intermediate [i3]. The latter decomposes via atomic hydrogen loss through a loose exit transition state with atomic hydrogen loss perpendicularly to the plane of the decomposing complex (sideways scattering) in a slightly exoergic reaction (experimentally: $-12 \pm 11$ kJ mol$^{-1}$; computationally: -1 kJ $\pm$ 3 kJ mol$^{-1}$). The silylidyne with D4-methylacetylene system exposed further details of the reaction mechanism and identified solely

an atomic hydrogen from the Si-H moiety yields eventually the aromatic 2-methyl-1-silacycloprop-2-enylidene molecule ($SiC_3H_4$). The formation of the 2-methyl-1-sila-cycloprop-2-enylidene molecule under single collision conditions enhances our knowledge towards the organosilicon formation in the bimolecular gas phase reaction, and further contributes to the completion of neutral-reaction reaction schemes of organosilicon formation in the physical organic chemistry as well as the astrochemical environments.

**Supporting Information**

Table S1: Zero-point vibration-corrected relative energies, point groups, symmetries of the electronic wave functions, and geometries of the reactants, products, intermediates, and transition states calculated at the ωB97X-V/cc-pVTZ level of theory. This information is available free of charge via the Internet at http://pubs.acs.org.

**Acknowledgements**

T. Y., B. B. D., and R. I. K. thank the National Science Foundation (NSF) for support under award CHE-1360658. L. W. B. thanks the NSF for an NSF Graduate Research Fellowship DGE-1106400, and M. H. G. thanks the NSF for support under award CHE-1363342.

## References


1. Balucani, N.; Skouteris, D.; Capozza, G.; Segoloni, E.; Casavecchia, P.; Alexander, M. H.; Capecchi, G.; Werner, H.-J. The Dynamics of the Prototype Abstraction Reaction Cl($^2P_{3/2,1/2}$)+ $H_2$: A Comparison of Crossed Molecular Beam Experiments with Exact Quantum Scattering Calculations on Coupled ab initio Potential Energy Surfaces. *Phys. Chem. Chem. Phys.* **2004,** *6*, 5007-5017.
2. Skouteris, D.; Werner, H.-J.; Aoiz, F. J.; Banares, L.; Castillo, J. F.; Menéndez, M.; Balucani, N.; Cartechini, L.; Casavecchia, P. Experimental and Theoretical Differential Cross Sections for the Reactions Cl + $H_2$/$D_2$. *J. Chem. Phys.* **2001,** *114*, 10662-10672.
3. Lee, S.-H.; Dong, F.; Liu, K. A Crossed-beam Study of the F + HD→ HF + D Reaction: The Resonance-mediated Channel. *J. Chem. Phys.* **2006,** *125*, 133106.
4. Bean, B. D.; Ayers, J. D.; Fernández-Alonso, F.; Zare, R. N. State-resolved Differential and Integral Cross Sections for the Reaction H + $D_2$ → HD(v'=3, *j'*=0-7) + D at 1.64 eV Collision Energy. *J. Chem. Phys.* **2002,** *116*, 6634-6639.
5. Balucani, N.; Capozza, G.; Segoloni, E.; Russo, A.; Bobbenkamp, R.; Casavecchia, P.; Gonzalez-Lezana, T.; Rackham, E. J.; Bañares, L.; Aoiz, F. J. Dynamics of the C($D_1$)+ $D_2$ Reaction: A Comparison of Crossed Molecular-beam Experiments with Quasiclassical Trajectory and Accurate Statistical Calculations. *J. Chem. Phys.* **2005,** *122*, 234309.
6. Balucani, N.; Casavecchia, P.; Aoiz, F. J.; Banares, L.; Launay, J.-M.; Bussery-Honvault, B.; Honvault, P. Dynamics of the C($^1$D)+ $H_2$ Reaction: A Comparison of Crossed Molecular Beam Experiments with Quantum Mechanical and Quasiclassical Trajectory Calculations on the First Two Singlet ($1^1$A' and $1^1$A") Potential Energy Surfaces. *Mol. Phys.* **2010,** *108*, 373-380.
7. Balucani, N.; Alagia, M.; Cartechini, L.; Casavecchia, P.; Volpi, G. G.; Pederson, L. A.; Schatz, G. C. Dynamics of the N($^2$D)+ $D_2$ Reaction from Crossed-Beam and Quasiclassical Trajectory Studies. *J. Phys. Chem. A* **2001,** *105*, 2414-2422.
8. Balucani, N.; Cartechini, L.; Capozza, G.; Segoloni, E.; Casavecchia, P.; Volpi, G. G.; Aoiz, F. J.; Bañares, L.; Honvault, P.; Launay, J.-M. Quantum Effects in the Differential Cross Sections for the Insertion Reaction N($^2$D)+ $H_2$. *Phys. Rev. Lett.* **2002,** *89*, 013201.
9. Balucani, N.; Casavecchia, P.; Banares, L.; Aoiz, F. J.; Gonzalez-Lezana, T.; Honvault, P.; Launay, J.-M. Experimental and Theoretical Differential Cross Sections for the N($^2$D)+ $H_2$ Reaction. *J. Phys. Chem. A* **2006,** *110*, 817-829.
10. Pederson, L. A.; Schatz, G. C.; Ho, T.-S.; Hollebeek, T.; Rabitz, H.; Harding, L. B.; Lendvay, G. Potential Energy Surface and Quasiclassical Trajectory Studies of the N($^2$D)+ $H_2$ Reaction. *J. Chem. Phys.* **1999,** *110*, 9091-9100.
11. Balucani, N.; Casavecchia, P.; Aoiz, F.; Banares, L.; Castillo, J.; Herrero, V. Dynamics of the O($^1$D) + $D_2$ Reaction: A Comparison Between Crossed Molecular Beam Experiments and Quasiclassical Trajectory Calculations on the Lowest Three Potential Energy Surfaces. *Mol. Phys.* **2005,** *103*, 1703-1714.
12. Gross, R.; Liu, X.; Suits, A. In *Crossed-Beam Imaging Studies of O($^3$P) Reaction Dynamics*, Abstracts of Papers of the American Chemical Society, American Chemical Society, 1155 16th St., NW, Washington, DC 20036 USA: 2002; C61-C61.
13. Lee, S.-H.; Liu, K. Direct Mapping of Insertion Reaction Dynamics: S($^1$D) + $H_2$ → SH + H. *Appl. Phys. B* **2000,** *71*, 627-633.
14. Maiti, B.; Schatz, G. C.; Lendvay, G. Importance of Intersystem Crossing in the S($^3$P, $^1$D) + $H_2$ → SH + H Reaction. *J. Phys. Chem. A* **2004,** *108*, 8772-8781.
15. Li, J.; Xie, C.; Ma, J.; Wang, Y.; Dawes, R.; Xie, D.; Bowman, J. M.; Guo, H. Quasi-Classical Trajectory Study of the HO + CO → H+ $CO_2$ Reaction on a New ab Initio Based Potential Energy Surface. *J. Phys. Chem. A* **2012,** *116*, 5057-5067.

16. Alagia, M.; Balucani, N.; Casavecchia, P.; Stranges, D.; Volpi, G. G. Reactive Scattering of Atoms and Radicals. *J. Chem. Soc., Faraday Trans.* **1995,** *91*, 575-596.
17. Liu, K.; Wagner, A. *The Chemical Dynamics and Kinetics of Small Radicals*; World Scientific: **1995**.
18. Strazisar, B. R.; Lin, C.; Davis, H. F. Mode-specific Energy Disposal in the Four-atom Reaction OH+ $D_2$ → HOD + D. *Science* **2000,** *290*, 958-961.
19. Alagia, M.; Balucani, N.; Casavecchia, P.; Stranges, D.; Volpi, G. G. Crossed Beam Studies of Four-atom Reactions: The dynamics of OH + $D_2$. *J. Chem. Phys.* **1993,** *98*, 2459-2462.
20. Takayanagi, T.; Schatz, G. C. Reaction Dynamics Calculations for the CN+ $H_2$ → HCN + H Reaction: Applications of the Rotating-bond Approximation. *J. Chem. Phys.* **1997,** *106*, 3227-3236.
21. Park, W. K.; Park, J.; Park, S. C.; Braams, B. J.; Chen, C.; Bowman, J. M. Quasiclassical Trajectory Calculations of the Reaction C + $C_2H_2$ → *I*-$C_3H$, *c*$C_3H$ + H, $C_3$ + $H_2$ using Full-dimensional Triplet and Singlet Potential Energy Surfaces. *J. Chem. Phys.* **2006,** *125*, 081101.
22. Zhang, B.; Liu, K.; Czakó, G.; Bowman, J. M. Translational Energy Dependence of the Cl + $CH_4$ ($v_b$ = 0, 1) Reactions: A Joint Crossed-beam and Quasiclassical Trajectory Study. *Mol. Phys.* **2012,** *110*, 1617-1626.
23. Czakó, G.; Bowman, J. M. Dynamics of the Reaction of Methane with Chlorine Atom on an Accurate Potential Energy Surface. *Science* **2011,** *334*, 343-346.
24. Czako´, G. b.; Shuai, Q.; Liu, K.; Bowman, J. M. Communication: Experimental and Theoretical Investigations of the Effects of the Reactant Bending Excitations in the F+ $CHD_3$ Reaction. *J. Chem. Phys.* **2010,** *133*, 131101.
25. Wang, F.; Liu, K. Experimental Signatures for a Resonance-mediated Reaction of Bend-excited $CD_4$($v_b$ = 1) with Fluorine Atoms. *J. Phys. Chem. Lett.* **2011,** *2*, 1421-1425.
26. Kawamata, H.; Liu, K. Imaging the Nature of the Mode-specific Chemistry in the Reaction of Cl Atom with Antisymmetric Stretch-excited $CH_4$. *J. Chem. Phys.* **2010,** *133*, 124304-124304.
27. Bowman, J. M.; Czako, G.; Fu, B. High-dimensional ab initio Potential Energy Surfaces for Reaction Dynamics Calculations. *Phys. Chem. Chem. Phys.* **2011,** *13*, 8094-8111.
28. Parker, D. S.; Balucani, N.; Stranges, D.; Kaiser, R. I.; Mebel, A. A Crossed Beam and ab Initio Investigation on the Formation of Boronyldiacetylene (HCCCC$^{11}$BO; $X^1\Sigma^+$) via the Reaction of the Boron Monoxide Radical ($^{11}$BO; $X^2\Sigma^+$) with Diacetylene ($C_4H_2$; $X^1\Sigma_g^+$). *J. Phys. Chem. A* **2013,** *117*, 8189-8198.
29. Maity, S.; Parker, D. S.; Dangi, B. B.; Kaiser, R. I.; Fau, S.; Perera, A.; Bartlett, R. J. A Crossed Molecular Beam and Ab-Initio Investigation of the Reaction of Boron Monoxide (BO; $X^2\Sigma^+$) with Methylacetylene ($CH_3CCH$; $X^1A_1$): Competing Atomic Hydrogen and Methyl Loss Pathways. *J. Phys. Chem. A* **2013,** *117*, 11794-11807.
30. Parker, D. S.; Dangi, B. B.; Balucani, N.; Stranges, D.; Mebel, A. M.; Kaiser, R. I. Gas-Phase Synthesis of Phenyl Oxoborane ($C_6H_5BO$) via the Reaction of Boron Monoxide with Benzene. *J. Org. Chem.* **2013,** *78*, 11896-11900.
31. Kaiser, R. I.; Maity, S.; Dangi, B. B.; Su, Y.-S.; Sun, B.; Chang, A. H. A Crossed Molecular Beam and ab initio Investigation of the Exclusive Methyl Loss Pathway in the Gas Phase Reaction of Boron Monoxide (BO; $X^2\Sigma^+$) with Dimethylacetylene ($CH_3CCCH_3$; $X^1A_{1g}$). *Phys. Chem. Chem. Phys.* **2014,** *16*, 989-997.
32. Parker, D.; Mebel, A.; Kaiser, R. The Role of Isovalency in the Reactions of the Cyano (CN), Boron Monoxide (BO), Silicon Nitride (SiN), and Ethynyl ($C_2H$) Radicals with Unsaturated Hydrocarbons Acetylene ($C_2H_2$) and Ethylene ($C_2H_4$). *Chem. Soc. Rev.* **2014,** *43*, 2701-2713.
33. Maity, S.; Dangi, B. B.; Parker, D. S.; Kaiser, R. I.; An, Y.; Sun, B.-J.; Chang, A. H. Combined Crossed Molecular Beam and ab Initio Investigation of the Multichannel Reaction of Boron Monoxide (BO; $X^2\Sigma^+$) with Propylene ($CH_3CHCH_2$; $X^1A'$): Competing Atomic Hydrogen and Methyl Loss Pathways. *J. Phys. Chem. A* **2014,** *118*, 9632-9645.

34. Maity, S.; Dangi, B. B.; Parker, D. S.; Kaiser, R. I.; Lin, H.-M.; Sun, B.-J.; Chang, A. Combined Crossed Molecular Beam and Ab Initio Investigation of the Reaction of Boron Monoxide (BO; $X^2\Sigma^+$) with 1,3-Butadiene ($CH_2CHCHCH_2$; $X^1A_g$) and Its Deuterated Counterparts. *J. Phys. Chem. A* **2015,** *119*, 1094-1107.
35. Maity, S.; Parker, D. S.; Kaiser, R. I.; Ganoe, B.; Fau, S.; Perera, A.; Bartlett, R. J. Gas-Phase Synthesis of Boronylallene ($H_2CCCH(BO)$) under Single Collision Conditions: A Crossed Molecular Beams and Computational Study. *J. Phys. Chem. A* **2014,** *118*, 3810-3819.
36. Yang, T.; Parker, D. S.; Dangi, B. B.; Kaiser, R. I.; Stranges, D.; Su, Y.-H.; Chen, S.-Y.; Chang, A. H.; Mebel, A. M. Directed Gas-Phase Formation of the Ethynylsulfidoboron Molecule. *J. Am. Chem. Soc.* **2014,** *136*, 8387-8392.
37. Yang, T.; Dangi, B. B.; Parker, D. S.; Kaiser, R. I.; An, Y.; Chang, A. H. A Combined Crossed Molecular Beams and ab initio Investigation on the Formation of Vinylsulfidoboron ($C_2H_3{}^{11}B^{32}S$). *Phys. Chem. Chem. Phys.* **2014,** *16*, 17580-17587.
38. Maksyutenko, P.; Zhang, F.; Gu, X.; Kaiser, R. I. A Crossed Molecular Beam Study on the Reaction of Methylidyne Radicals [$CH(X^2\Pi)$] with Acetylene [$C_2H_2(X^1\Sigma_g^+)$] — Competing $C_3H_2$ + H and $C_3H$ + $H_2$ Channels. *Phys. Chem. Chem. Phys.* **2011,** *13*, 240-252.
39. Kaiser, R. I.; Gu, X.; Zhang, F.; Maksyutenko, P. Crossed Beam Reactions of Methylidyne [$CH(X^2\Pi)$] with D2-acetylene [$C_2D_2$ ($X^1\Sigma_g^+$)] and of D1-methylidyne [$CD(X^2\Pi)$] with Acetylene [$C_2H_2(X^1\Sigma_g^+)$]. *Phys. Chem. Chem. Phys.* **2012,** *14*, 575-588.
40. Liu, K.; Macdonald, R. G. State-to-state Reaction Dynamics: A Crossed Molecular Beam Study of the Reaction $CH(^2\Pi_{1/2}; N = 1) + D_2 \rightarrow CD(^2\Pi_{1/2, 3/2}; N') + HD$. *J. Chem. Phys.* **1988,** *89*, 4443-4444.
41. Macdonald, R. G.; Liu, K. A Crossed-beam Study of the State-resolved Dynamics of $CH(X^2\Pi)$ + $D_2$. II. The Isotopic Exchange Channel. *J. Chem. Phys.* **1990,** *93*, 2443-2459.
42. Zhang, F.; Maksyutenko, P.; Kaiser, R. I. Chemical Dynamics of the $CH(X^2\Pi) + C_2H_4(X^1A_{1g})$, $CH(X^2\Pi) + C_2D_4(X^1A_{1g})$, and $CD(X^2\Pi) + C_2H_4(X^1A_{1g})$ Reactions Studied under Single Collision Conditions. *Phys. Chem. Chem. Phys.* **2012,** *14*, 529-537.
43. Ohoyama, H.; Yamakawa, K.; Oda, R.; Nagamachi, Y.; Kasai, T. Rotationally Correlated Reactivity in the $CH(\nu = 0, J, Fi) + O_2 \rightarrow OH(A) + CO$ Reaction. *J. Chem. Phys.* **2011,** *134*, 114306.
44. Takezaki, M.; Ohoyama, H.; Kasai, T.; Kuwata, K. Formation of the State-Selected CH Radical Beam and its Application to the CH + NO Reaction. *Laser Chem.* **1995,** *15*, 113-122.
45. Ohoyama, H.; Nagamachi, Y.; Yamakawa, K.; Kasai, T. Collision Energy Dependence of the Rotational-state-resolved Cross Section in the CH ($\nu$ = 0, J, $F_i$) + $O_2 \rightarrow$ OH(A) + CO Reaction. *Phys. Chem. Chem. Phys.* **2009,** *11*, 10281-10285.
46. Gu, X.; Zhang, F.; Kaiser, R. I. Reaction Dynamics on the Formation of 1- and 3-Cyanopropylene in the Crossed Beams Reaction of Ground-state Cyano Radicals (CN) with Propylene ($C_3H_6$) and Its Deuterated Isotopologues. *J. Phys. Chem. A* **2008,** *112*, 9607-9613.
47. Morales, S. B.; Bennett, C. J.; Le Picard, S. D.; Canosa, A.; Sims, I. R.; Sun, B.; Chen, P.; Chang, A. H.; Kislov, V. V.; Mebel, A. M. A Crossed Molecular Beam, Low-Temperature Kinetics, and Theoretical Investigation of the Reaction of the Cyano Radical (CN) with 1,3-Butadiene ($C_4H_6$). A Route to Complex Nitrogen-Bearing Molecules in Low-Temperature Extraterrestrial Environments. *Astrophys. J.* **2011,** *742*, 26.
48. Kaiser, R. I.; Mebel, A. M. On the Formation of Polyacetylenes and Cyanopolyacetylenes in Titan's Atmosphere and Their Role in Astrobiology. *Chem. Soc. Rev.* **2012,** *41*, 5490-5501.
49. Estillore, A. D.; Visger, L. M.; Kaiser, R. I.; Suits, A. G. Crossed-Beam Imaging of the H Abstraction Channel in the Reaction of CN with 1-Pentene. *J. Phys. Chem. Lett.* **2010,** *1*, 2417-2421.
50. Huang, C.; Li, W.; Estillore, A. D.; Suits, A. G. Dynamics of CN + Alkane Reactions by Crossed-beam Dc Slice Imaging. *J. Chem. Phys.* **2008,** *129*, 074301.

51. Wang, J. H.; Liu, K.; Schatz, G. C.; ter Horst, M. Experimental and Theoretical Angular and Translational Energy Distributions for the Reaction CN + D2 → DCN + D. *J. Chem. Phys.* **1997,** *107*, 7869-7875.
52. Macdonald, R. G.; Argonne, K. L.; Sonnenfroh, D. M.; Liu, D.-J. Crossed-beam Studies of Radical Reaction Dynamics. *Can. J. Chem.* **1994,** *72*, 660-672.
53. Balucani, N.; Leonori, F.; Petrucci, R.; Wang, X.; Casavecchia, P.; Skouteris, D.; Albernaz, A. F.; Gargano, R. A Combined Crossed Molecular Beams and Theoretical Study of the Reaction CN + $C_2H_4$. *Chem. Phys.* **2015,** *449*, 34-42.
54. Casavecchia, P.; Balucani, N.; Cartechini, L.; Capozza, G.; Bergeat, A.; Volpi, G. G. Crossed Beam Studies of Elementary Reactions of N and C Atoms and CN Radicals of Importance in Combustion. *Faraday Discuss.* **2002,** *119*, 27-49.
55. Leonori, F.; Petrucci, R.; Wang, X.; Casavecchia, P.; Balucani, N. A Crossed Beam Study of the Reaction CN + $C_2H_4$ at a High Collision Energy: The Opening of a New Reaction Channel. *Chem. Phys. Lett.* **2012,** *553*, 1-5.
56. Kaiser, R. I.; Balucani, N. The Formation of Nitriles in Hydrocarbon-rich Atmospheres of Planets and Their Satellites: Laboratory Investigations by the Crossed Molecular Beam Technique. *Acc. Chem. Res.* **2001,** *34*, 699-706.
57. Leonori, F.; Hickson, K. M.; Le Picard, S. D.; Wang, X.; Petrucci, R.; Foggi, P.; Balucani, N.; Casavecchia, P. Crossed-beam Universal-detection Reactive Scattering of Radical Beams Characterized by Laser-induced-fluorescence: The Case of $C_2$ and CN. *Mol. Phys.* **2010,** *108*, 1097-1113.
58. Bennett, C. J.; Morales, S. B.; Le Picard, S. D.; Canosa, A.; Sims, I. R.; Shih, Y.; Chang, A.; Gu, X.; Zhang, F.; Kaiser, R. I. A Chemical Dynamics, Kinetics, and Theoretical Study on the Reaction of the Cyano Radical (CN; $X^2\Sigma^+$) with Phenylacetylene ($C_6H_5CCH$; $X^1A_1$). *Phys. Chem. Chem. Phys.* **2010,** *12*, 8737-8749.
59. Zhang, F.; Gu, X.; Kaiser, R. I. In *PHYS 730-Chemical Dynamics of Bimolecular Reactions of Cyano Radicals with Unsaturated Hydrocarbons Toward the Stepwise Build-up of the Aerosol Layer in Titan's Atmosphere*, Abstracts of Papers of the American Chemical Society, AMER CHEMICAL SOC 1155 16TH ST, NW, WASHINGTON, DC 20036 USA: 2008.
60. Balucani, N.; Asvany, O.; Osamura, Y.; Huang, L.; Lee, Y.; Kaiser, R. Laboratory Investigation on the Formation of Unsaturated Nitriles in Titan's Atmosphere. *Planet. Space Sci.* **2000,** *48*, 447-462.
61. Kaiser, R. I.; Maksyutenko, P.; Ennis, C.; Zhang, F.; Gu, X.; Krishtal, S. P.; Mebel, A. M.; Kostko, O.; Ahmed, M. Untangling the Chemical Evolution of Titan's Atmosphere and Surface – From Homogeneous to Heterogeneous Chemistry. *Faraday Discuss.* **2010,** *147*, 429-478.
62. Kaiser, R.; Yamada, M.; Osamura, Y. A Crossed Beam and ab Initio Investigation of the Reaction of Hydrogen Sulfide, $H_2S(X^1A_1)$, with Dicarbon Molecules, $C_2$ ($X^1\Sigma_g^+$). *J. Phys. Chem. A* **2002,** *106*, 4825-4832.
63. Gu, X.; Guo, Y.; Zhang, F.; Mebel, A. M.; Kaiser, R. I. A Crossed Molecular Beams Study of the Reaction of Dicarbon Molecules with Benzene. *Chem. Phys. Lett.* **2007,** *436*, 7-14.
64. Dangi, B. B.; Maity, S.; Kaiser, R. I.; Mebel, A. M. A Combined Crossed Beam and Ab Initio Investigation of the Gas Phase Reaction of Dicarbon Molecules ($C_2$; $X^1\Sigma_g^+/a^3\Pi_u$) with Propene ($C_3H_6$; $X^1A'$): Identification of the Resonantly Stabilized Free Radicals 1-and 3-Vinylpropargyl. *J. Phys. Chem. A* **2013,** *117*, 11783-11793.
65. Parker, D. S.; Maity, S.; Dangi, B. B.; Kaiser, R. I.; Landera, A.; Mebel, A. M. Understanding the Chemical Dynamics of the Reactions of Dicarbon with 1-Butyne, 2-Butyne, and 1, 2-Butadiene – Toward the Formation of Resonantly Stabilized Free Radicals. *Phys. Chem. Chem. Phys.* **2014,** *16*, 12150-12163.
66. Dangi, B. B.; Parker, D. S.; Kaiser, R. I.; Belisario-Lara, D.; Mebel, A. M. An Experimental and Theoretical Investigation of the Formation of $C_7H_7$ Isomers in the Bimolecular Reaction of Dicarbon Molecules with 1,3-Pentadiene. *Chem. Phys. Lett.* **2014,** *607*, 92-99.

67. Dangi, B. B.; Parker, D. S.; Yang, T.; Kaiser, R. I.; Mebel, A. M. Gas-Phase Synthesis of the Benzyl Radical ($C_6H_5CH_2$). *Angew. Chem. Int. Edit.* **2014,** *53*, 4608-4613.
68. Gu, X.; Kaiser, R.; Mebel, A.; Kislov, V.; Klippenstein, S.; Harding, L.; Liang, M.; Yung, Y. A Crossed Molecular Beams Study on the Formation of the Exotic Cyanoethynyl Radical in Titan's Atmosphere. *Astrophys. J.* **2009,** *701*, 1797-2803.
69. Kaiser, R.; Goswami, M.; Maksyutenko, P.; Zhang, F.; Kim, Y.; Landera, A.; Mebel, A. M. A Crossed Molecular Beams and ab initio Study on the Formation of $C_6H_3$ Radicals. An Interface between Resonantly Stabilized and Aromatic Radicals. *J. Phys. Chem. A* **2011,** *115*, 10251-10258.
70. Zhang, F.; Jones, B.; Maksyutenko, P.; Kaiser, R. I.; Chin, C.; Kislov, V. V.; Mebel, A. M. Formation of the Phenyl Radical [$C_6H_5(X^2A_1)$] under Single Collision Conditions: A Crossed Molecular Beam and ab initio Study. *J. Am. Chem. Soc.* **2010,** *132*, 2672-2683.
71. Sun, Y.-L.; Huang, W.-J.; Chin, C.-H.; Lee, S.-H. Dynamics of the Reaction of $C_2$ with $C_6H_2$: An Implication for the Formation of Interstellar $C_8H$. *J. Chem. Phys.* **2014,** *141*, 194305.
72. Lee, S.-H.; Huang, W.-J.; Lin, Y.-C.; Chin, C.-H. Searching for Interstellar Molecule Butatrienylidene in Reaction $C_2 + C_2H_4$. *Astrophys. J.* **2012,** *759*, 75.
73. Leonori, F.; Petrucci, R.; Hickson, K. M.; Segoloni, E.; Balucani, N.; Le Picard, S. D.; Foggi, P.; Casavecchia, P. Crossed Molecular Beam Study of Gas Phase Reactions Relevant to the Chemistry of Planetary Atmospheres: the Case of $C_2 + C_2H_2$. *Planet. Space Sci.* **2008,** *56*, 1658-1673.
74. Balucani, N.; Leonori, F.; Petrucci, R.; Hickson, K. M.; Casavecchia, P. Crossed Molecular Beam Studies of C($^3$P, $^1$D) and $C_2(X^1\Sigma_g^+, a^3\Pi_u)$ Reactions with Acetylene. *Phys. Scr.* **2008,** *78*, 058117.
75. Ortiz-Suárez, M.; Witinski, M. F.; Davis, H. F. Reactive Quenching of OH($A^2\Sigma^+$) by $D_2$ Studied using Crossed Molecular Beams. *J. Chem. Phys.* **2006,** *124*, 201106.
76. Zhang, B.; Shiu, W.; Liu, K. Imaging the Reaction Dynamics of OH + $CD_4$. 2. Translational Energy Dependencies. *J. Phys. Chem. A* **2005,** *109*, 8983-8988.
77. Kirste, M.; Wang, X.; Schewe, H. C.; Meijer, G.; Liu, K.; van der Avoird, A.; Janssen, L. M.; Gubbels, K. B.; Groenenboom, G. C.; van de Meerakker, S. Y. Quantum-state Resolved Bimolecular Collisions of Velocity-controlled OH with NO Radicals. *Science* **2012,** *338*, 1060-1063.
78. Sonnenfroh, D. M.; Macdonald, R. G.; Liu, K. A Crossed-beam study of the State-resolved Integral Cross Sections for the Inelastic Scattering of OH ($X^2\Pi$) with CO and $N_2$. *J. Chem. Phys.* **1991,** *94*, 6508-6518.
79. Laganà, A.; Garcia, E.; Paladini, A.; Casavecchia, P.; Balucani, N. The Last Mile of Molecular Reaction Dynamics Virtual Experiments: The Case of the OH(N = 1-10) + CO(j = 0-3) Reaction. *Faraday Discuss.* **2012,** *157*, 415-436.
80. Alagia, M.; Balucani, N.; Casavecchia, P.; Stranges, D.; Volpi, G. G. Crossed Beam Studies of Four-atom Reactions: The Dynamics of OH + CO. *J. Chem. Phys.* **1993,** *98*, 8341-8344.
81. van Beek, M.; Ter Meulen, J. The Effect of Molecular Orientation in Collisions of OH with CO and $N_2$. *J. Chem. Phys.* **2001,** *115*, 1843-1852.
82. Alagia, M.; Balucani, N.; Casavecchia, P.; Stranger, D.; Volpi, G.; Clary, D.; Kliesch, A.; Werner, H.-J. The Dynamics of the Reaction OH + $D_2$ → HOD+ D: Crossed Beam Experiments and Quantum Mechanical Scattering Calculations on ab initio Potential Energy Surfaces. *Chem. Phys.* **1996,** *207*, 389-409.
83. Xiao, C.; Xu, X.; Liu, S.; Wang, T.; Dong, W.; Yang, T.; Sun, Z.; Dai, D.; Zhang, D. H.; Yang, X. Experimental and Theoretical Differential Cross Sections for a Four-atom Reaction: HD + OH → $H_2O$+ D. *Science* **2011,** *333*, 440-442.
84. Kirste, M.; Scharfenberg, L.; Kłos, J.; Lique, F.; Alexander, M. H.; Meijer, G.; van de Meerakker, S. Y. Low-energy Inelastic Collisions of OH Radicals with He Atoms and $D_2$ Molecules. *Phys. Rev. A* **2010,** *82*, 042717.
85. Che, D.-C.; Matsuo, T.; Yano, Y.; Bonnet, L.; Kasai, T. Negative Collision Energy Dependence of Br Formation in the OH + HBr Reaction. *Phys. Chem. Chem. Phys.* **2008,** *10*, 1419-1423.

86. Cireasa, D.; van Beek, M.; Moise, A.; ter Meulen, J. Inelastic State-to-state Scattering of OH ($^2\Pi_{3/2}$, $J = 3/2, f$) by HCl. *J. Chem. Phys.* **2005**, 074319.
87. Parker, D. S.; Wilson, A. V.; Kaiser, R. I.; Mayhall, N. J.; Head-Gordon, M.; Tielens, A. G. On the Formation of Silacyclopropenylidene (c-$SiC_2H_2$) and its Role in the Organosilicon Chemistry in the Interstellar Medium. *Astrophys. J.* **2013,** *770*, 33.
88. Astrochymist, T. The Astrochymist - Resources for Astrochemists and Interested Bystanders. http://www.astrochymist.org/astrochymist_ism.html.
89. Marvel, K. B. No Methane Here. The HCN Puzzle: Searching for $CH_3OH$ and $C_2H$ in Oxygen-rich Stars. *Astro. J.* **2005,** *130*, 261-268.
90. MacKay, D.; Charnley, S. The Silicon Chemistry of IRC+ 10° 216. *Mon. Not. R. Astron. Soc.* **1999,** *302*, 793-800.
91. Wakelam, V.; Smith, I.; Herbst, E.; Troe, J.; Geppert, W.; Linnartz, H.; Öberg, K.; Roueff, E.; Agúndez, M.; Pernot, P. Reaction Networks for Interstellar Chemical Modelling: Improvements and Challenges. *Space Sci. Rev.* **2010,** *156*, 13-72.
92. Howe, D.; Millar, T. The Formation of Carbon Chain Molecules in IRC+ 10216. *Mon. Not. R. Astron. Soc.* **1990,** *244*, 444-449.
93. Willacy, K.; Cherchneff, I. Silicon and Sulphur Chemistry in the Inner Wind of IRC+ 10216. *Astron. Astrophys.* **1998,** *330*, 676-684.
94. Millar, T.; Herbst, E. A New Chemical Model of the Circumstellar Envelope Surrounding IRC+ 10216. *Astron. Astrophys.* **1994,** *288*, 561-571.
95. Millar, T.; Herbst, E.; Bettens, R. Large Molecules in the Envelope Surrounding IRC+ 10216. *Mon. Not. R. Astron. Soc.* **2000,** *316*, 195-203.
96. Brown, J.; Millar, T. Modelling Enhanced Density Shells in the Circumstellar Envelope of IRC+ 10216. *Mon. Not. R. Astron. Soc.* **2003,** *339*, 1041-1047.
97. Ziurys, L.; Halfen, D.; Woolf, N. In *Establishing the Synthetic Contingencies for Life: Following the Carbon from AGB Stars to Planetary Surfaces*, Bioastronomy 2007: Molecules, Microbes and Extraterrestrial Life, 2009; 59.
98. Kaiser, R. I.; Osamura, Y. Laboratory Studies on the Infrared Absorptions of Hydrogenated Carbon-silicon Clusters: Directing the Identification of Organometallic $SiCH_x$ species toward IRC+ 10216. *Astrophys. J.* **2005,** *630*, 1217-1223.
99. Wang, H. J.; Schleyer, P. v. R.; Wu, J. I.; Wang, Y.; Wang, H. J. A Study of Aomatic Three Membered Rings. *Int. J. Quant. Chem.* **2011,** *111*, 1031-1038.
100. von Schleyer, P. R., The Contrasting Strain Energies of Small Ring Carbon and Silicon Rings. The Relationship with free Radical Energies. In *Substituent Effects in Radical Chemistry*, Springer: 1986; pp 69-81.
101. Sander, W.; Trommer, M.; Patyk, A. Oxidation of Silenes and Silylenes: Matrix Isolation of Unusual Silicon Species. *Organosilicon Chemistry Set: From Molecules to Materials* **2008**, 86-94.
102. von Ragué Schleyer, P.; Jiao, H.; Goldfuss, B.; Freeman, P. K. Aromaticity and Antiaromaticity in Five‐Membered $C_4H_4X$ Ring Systems: "Classical" and "Magnetic" Concepts May Not Be "Orthogonal". *Angew. Chem. Int. Edit.* **1995,** *34*, 337-340.
103. Schleyer, P. v. R.; Kost, D. A Comparison of the Energies of Double Bonds of Second-row Elements with Carbon and Silicon. *J. Am. Chem. Soc.* **1988,** *110*, 2105-2109.
104. Gu, X.; Kaiser, R. I. Reaction Dynamics of Phenyl Radicals in Extreme Environments: A Crossed Molecular Beam Study. *Acc. Chem. Res.* **2008,** *42*, 290-302.
105. Guo, Y.; Gu, X.; Kawamura, E.; Kaiser, R. I. Design of a Modular and Versatile Interlock System for Ultrahigh Vacuum Machines: A Crossed Molecular Beam Setup as a Case Study. *Rev. Sci. Instrum.* **2006,** *77*, 034701.
106. Gu, X.; Guo, Y.; Zhang, F.; Mebel, A. M.; Kaiser, R. I. Reaction Dynamics of Carbon-bearing Radicals in Circumstellar Envelopes of Carbon Stars. *Faraday Discuss.* **2006,** *133*, 245-275.

107. Zhang, F.; Kim, S.; Kaiser, R. I. A Crossed Molecular Beams Study of the Reaction of the Ethynyl Radical ($C_2H(X^2\Sigma^+)$) with Allene ($H_2CCCH_2$ ($X^1A_1$)). *Phys. Chem. Chem. Phys.* **2009,** *11*, 4707-4714.
108. Yang, T.; Dangi, B. B.; Maksyutenko, P.; Kaiser, R. I.; Bertels, L. W.; Head-Gordon, M. Combined Experimental and Theoretical Study on the Formation of the Elusive 2-Methyl-1-silacycloprop-2-enylidene Molecule under Single Collision Conditions via Reactions of the Silylidyne Radical (SiH; $X^2\Pi$) with Allene ($H_2CCCH_2$; $X^1A_1$) and D4-Allene ($D_2CCCD_2$; $X^1A_1$). *J. Phys. Chem. A* **2015,** *119*, 12562-12578.
109. Veron, M. Ph. D. thesis, University of California at Berkeley, Berkeley, California, 1981.
110. Weiss, M. S. Ph. D. thesis, University of California at Berkeley, Berkeley, California, 1986.
111. Kaiser, R. I.; Le, T. N.; Nguyen, T. L.; Mebel, A. M.; Balucani, N.; Lee, Y. T.; Stahl, F.; Schleyer, P. v. R.; Schaefer Iii, H. F. A Combined Crossed Molecular Beam and ab initio Investigation of $C_2$ and $C_3$ Elementary Reactions with Unsaturated Hydrocarbons—Pathways to Hydrogen Deficient Hydrocarbon Radicals in Combustion Flames. *Faraday Discuss.* **2002,** *119*, 51-66.
112. Levine, R. D.; Bernstein, R. B.; Lee, Y. T. Molecular Reaction Dynamics and Chemical Reactivity. *Phys. Today* **1988**, 90.
113. Kaiser, R.; Parker, D.; Zhang, F.; Landera, A.; Kislov, V.; Mebel, A. PAH Formation under Single Collision Conditions: Reaction of Phenyl Radical and 1, 3-Butadiene to Form 1, 4-Dihydronaphthalene. *J. Phys. Chem. A* **2012,** *116*, 4248-4258.
114. Mardirossian, N.; Head-Gordon, M. ωB97X-V: A 10-Parameter, Range-separated Hybrid, Generalized Gradient Approximation Density Functional with Nonlocal Correlation, Designed by a Survival-of-the-fittest Strategy. *Phys. Chem. Chem. Phys.* **2014,** *16*, 9904-9924.
115. Kendall, R. A.; Dunning Jr, T. H.; Harrison, R. J. Electron Affinities of the First-row Atoms Revisited. Systematic Basis Sets and Wave Functions. *J. Chem. Phys.* **1992,** *96*, 6796-6806.
116. Behn, A.; Zimmerman, P. M.; Bell, A. T.; Head-Gordon, M. Efficient Exploration of Reaction Paths via a Freezing String Method. *J. Chem. Phys.* **2011,** *135*, 224108.
117. Mallikarjun Sharada, S.; Zimmerman, P. M.; Bell, A. T.; Head-Gordon, M. Automated Transition State Searches without Evaluating the Hessian. *J. Chem. Theo. Comp.* **2012,** *8*, 5166-5174.
118. Baker, J. An Algorithm for the Location of Transition States. *J. Comp. Chem.* **1986,** *7*, 385-395.
119. Raghavachari, K.; Trucks, G. W.; Pople, J. A.; Head-Gordon, M. A Fifth-order Perturbation Comparison of Electron Correlation Theories. *Chem. Phys. Lett.* **1989,** *157*, 479-483.
120. Feyereisen, M.; Fitzgerald, G.; Komornicki, A. Use of Approximate Integrals in ab initio Theory. An Application in MP2 Energy Calculations. *Chem. Phys. Lett.* **1993,** *208*, 359-363.
121. Bernholdt, D. E.; Harrison, R. J. Large-scale Correlated Electronic Structure Calculations: The RI-MP2 Method on Parallel Computers. *Chem. Phys. Lett.* **1996,** *250*, 477-484.
122. Halkier, A.; Helgaker, T.; Jørgensen, P.; Klopper, W.; Koch, H.; Olsen, J.; Wilson, A. K. Basis-set Convergence in Correlated Calculations on Ne, $N_2$, and $H_2O$. *Chem. Phys. Lett.* **1998,** *286*, 243-252.
123. Shao, Y.; Gan, Z.; Epifanovsky, E.; Gilbert, A. T.; Wormit, M.; Kussmann, J.; Lange, A. W.; Behn, A.; Deng, J.; Feng, X. Advances in Molecular Quantum Chemistry Contained in the Q-Chem 4 Program Package. *Mol. Phys.* **2015,** *113*, 184-215.
124. Schriver, G. W.; Fink, M. J.; Gordon, M. S. Ab initio Calculations on Some $C_3SiH_4$ Isomers. *Organometallics* **1987,** *6*, 1977-1984.
125. Levine, R. D. *Molecular Reaction Dynamics*; Cambridge University Press: **2005**.
126. Herschbach, D. R. Reactive Collisions in Crossed Molecular Beams. *Discuss. Faraday Soc.* **1962,** *33*, 149-161.

Table 1. Crossed molecular beam studies of diatomic radicals with closed-shell molecules. Unless noted otherwise, all diatomic radical sources are pulsed.

| Chemical Name | Boron Monoxide | Boron Monosulfide | Methylidyne | Cyano | Dicarbon | Hydroxyl | Silicon Nitride | Silylidyne |
|---|---|---|---|---|---|---|---|---|
| Formula | BO | BS | CH/CD | CN | $C_2$ | OH | SiN | SiH/SiD |
| Electronic State | $X^2\Sigma^+$ | $X^2\Sigma^+$ | $X^2\Pi$ | $X^2\Sigma^+$ | $X^1\Sigma_g^+/a^3\Pi_u$ | $X^2\Pi/A^2\Sigma^+$ | $X^2\Sigma^+$ | $X^2\Pi$ |
| Reaction Partner with Generation Source | Ablation | Ablation | Photolysis<br>*DC Discharge* | Ablation<br>*RF Discharge(Continuous)*<br>**Photolysis** | Ablation<br>*RF Discharge(Continuous)*<br>**DC Discharge** | Photolysis<br>*RF Discharge(Continuous)*<br>**DC Discharge** | Ablation | Ablation<br>*Photolysis* |
| | Acetylene (HCCH)[32]<br>Ethylene ($H_2CCH_2$)[32]<br>Methylacetylene ($CH_3CCH$)[29]<br>Allene ($CH_2CCH_2$)[35]<br>Propylene ($CH_3CCH_2$)[33]<br>Diacetylene (HCCCCH)[28]<br>1,3-Butadiene ($CH_2CHCHCH_2$)[34]<br>2-Butyne ($CH_3CCCH_3$)[31]<br>Benzene ($C_6H_6$)[30] | Acetylene (HCCH)[36]<br>Ethylene ($H_2CCH_2$)[37] | Acetylene (HCCH)[38-39]<br>Ethylene ($H_2CCH_2$)[42]<br>Deuterium ($D_2$)[40-41]<br>*Oxygen($O_2$)[43, 45]*<br>*Nitric Oxide (NO)[44]* | Acetylene (HCCH)[32, 48, 56, 60-61]<br>Ethylene ($H_2CCH_2$)[32, 56, 60-61]<br>Methylacetylene ($CH_3CCH$)[48, 56, 60-61]<br>Allene ($CH_2CCH_2$)[56, 60-61]<br>Propylene($CH_3CCH_2$)[46]<br>Diacetylene (HCCCCH)[48, 61]<br>Vinylacetylene ($HCCC_2H_3$)[59]<br>1,3-Butadiene ($CH_2CHCHCH_2$)[47]<br>2-Butyne ($CH_3CCCH_3$)[56, 60]<br>Benzene ($C_6H_6$)[56, 60-61]<br>Phenylacetylene ($C_6H_5CCH$)[58]<br>Styrene ($C_6H_5C_2H_3$)<br>*Acetylene (HCCH)[54, 57]*<br>*Ethylene ($H_2CCH_2$)[53, 55]*<br>*Methylacetylene ($CH_3CCH$)[57]*<br>**1-Pentene ($CH_3CH_2CH_2CHCH_2$)[49]**<br>**Butane ($CH_3CH_2CH_2CH_3$)[50]**<br>**Pentane ($CH_3CH_2CH_2CH_2CH_3$)[50]**<br>**Hexane ($CH_3CH_2CH_2CH_2CH_2CH_3$)[50]**<br>**Cyclohexane($C_6H_{12}$)[50]**<br>**Deuterium($D_2$)[51]**<br>**Oxygen($O_2$)[52]** | Acetylene (HCCH)[61]<br>Ethylene ($H_2CCH_2$)[61]<br>Methylacetylene ($CH_3CCH$)[61]<br>Allene($H_2CCCH_2$)[61]<br>Propylene($CH_3CCH_2$)[64]<br>Diacetylene(HCCCCH)[61]<br>Vinylacetylene ($CH_2CHCCH$)[69]<br>1,3-Butadiene ($CH_2CHCHCH_2$)[70]<br>1,2-Butadiene ($CH_3CHCCH_2$)[65]<br>1-Butyne($CH_3CH_2CCH$)[65]<br>2-Butyne($CH_3CCCH_3$)[65]<br>1,3-Pentadiene ($CH_3CHCHCHCH_2$)[66]<br>Isoprene ($CH_2C(CH_3)CHCH_2$)[67]<br>Benzene($C_6H_6$)[61, 63]<br>Hydrogen Sulfide($H_2S$)[62]<br>Hydrogen Cyanide(HCN)[68]<br>*Acetylene (HCCH)[73-74]*<br>**Ethylene ($H_2CCH_2$)[72]**<br>**Triacetylene (HCCCCCCH)[71]** | Deuterium ($D_2$)[75, 84]<br>Hydrogen Deuteride (HD)[83]<br>D4-methane ($CD_4$)[76]<br>Nitric Oxide (NO)[77]<br>Carbon Monoxide (CO)[78]<br>Nitrogen($N_2$)[78]<br>*Hydrogen ($H_2$)[16]*<br>*Deuterium ($D_2$)[19, 82]*<br>*Carbon Monoxide (CO)[16, 79-80]*<br>**Carbon Monoxide (CO)[81]**<br>**Nitrogen($N_2$)[81]**<br>**Hydrogen Chloride (HCl)[86]**<br>**Hydrogen Bromide (HBr)[85]** | Acetylene (HCCH)[32]<br>Ethylene ($H_2CCH_2$)[32] | Acetylene (HCCH)[87]<br>*Allene ($H_2CCCH_2$)[108]* |

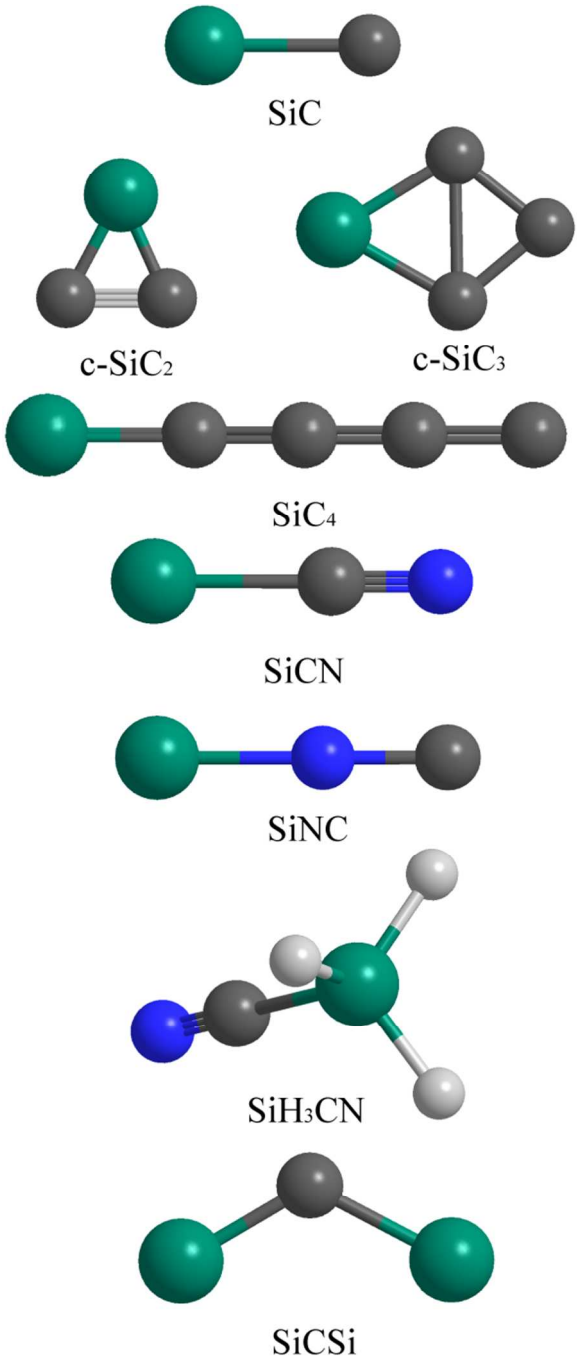


Figure 1. Silicon-carbon bearing molecules detected in the circumstellar envelopes so far.

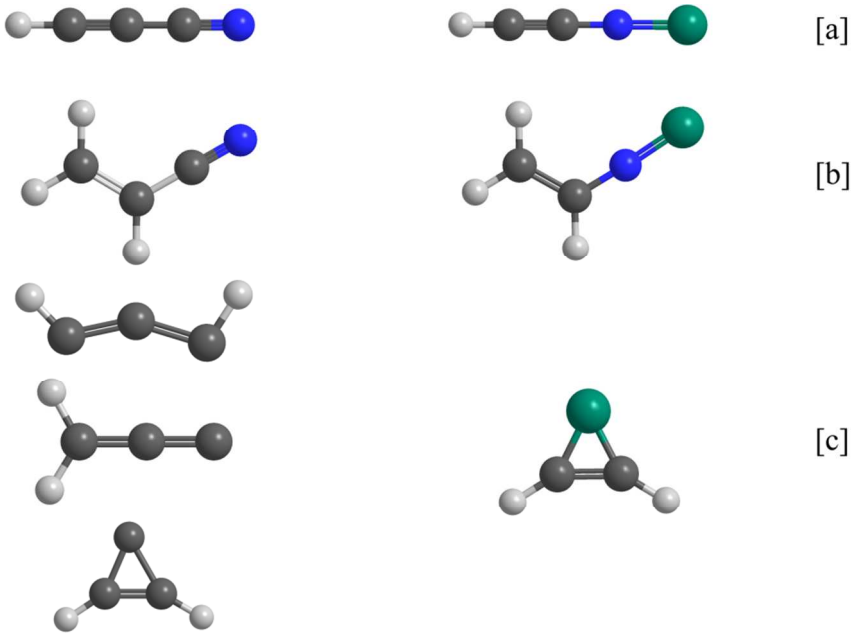


Figure 2. Left column: structures of products formed in bimolecular reactions of cyano (CN) [a/b] with acetylene ($C_2H_2$) and ethylene ($C_2H_4$), as well as methylidyne (CH) [c] with acetylene. Right column: Structures of products formed in bimolecular reactions of the isovalent silicon nitride (SiN) [a/b] and D1-silylidyne (SiD) [c] with the same unsaturated hydrocarbons, respectively.

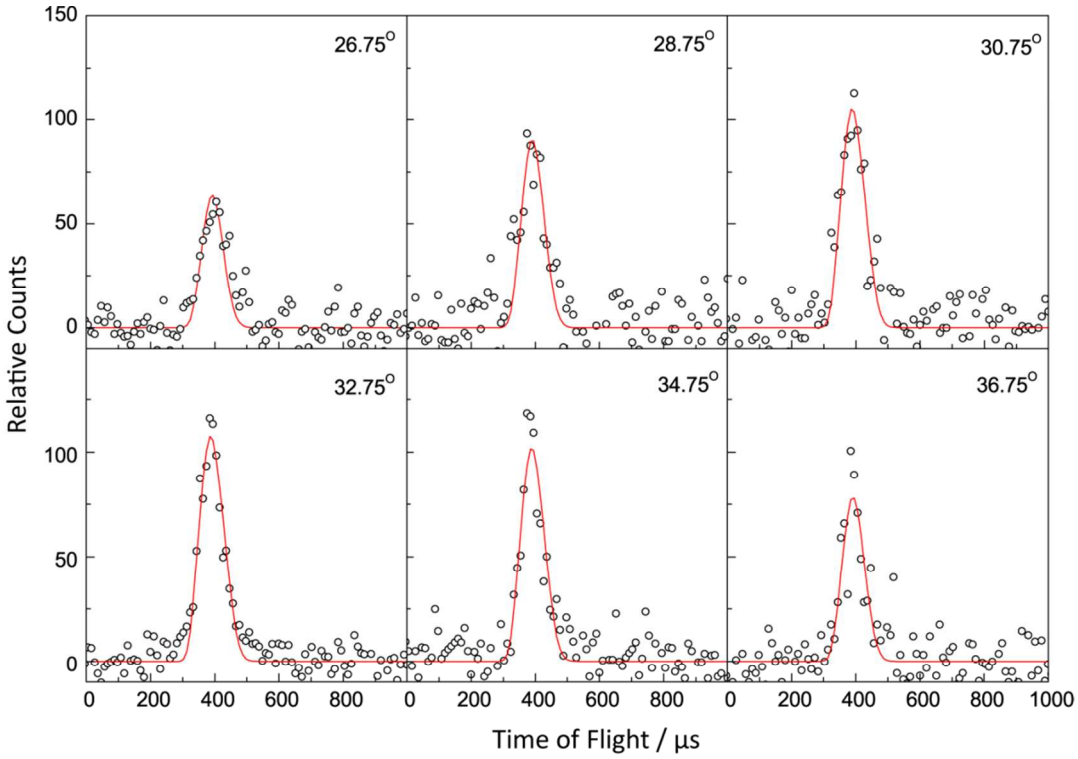


Figure 3. Selected time-of-flight (TOF) spectra recorded at a mass-to-charge ratio (*m/z*) of 68 ($SiC_3H_4^+$) for the reaction of the silylidyne radical (SiH; $X^2\Pi$) with methylacetylene ($CH_3CCH$; $X^1A_1$). The circles represent the experimental data, while the solid lines represent the best fits.

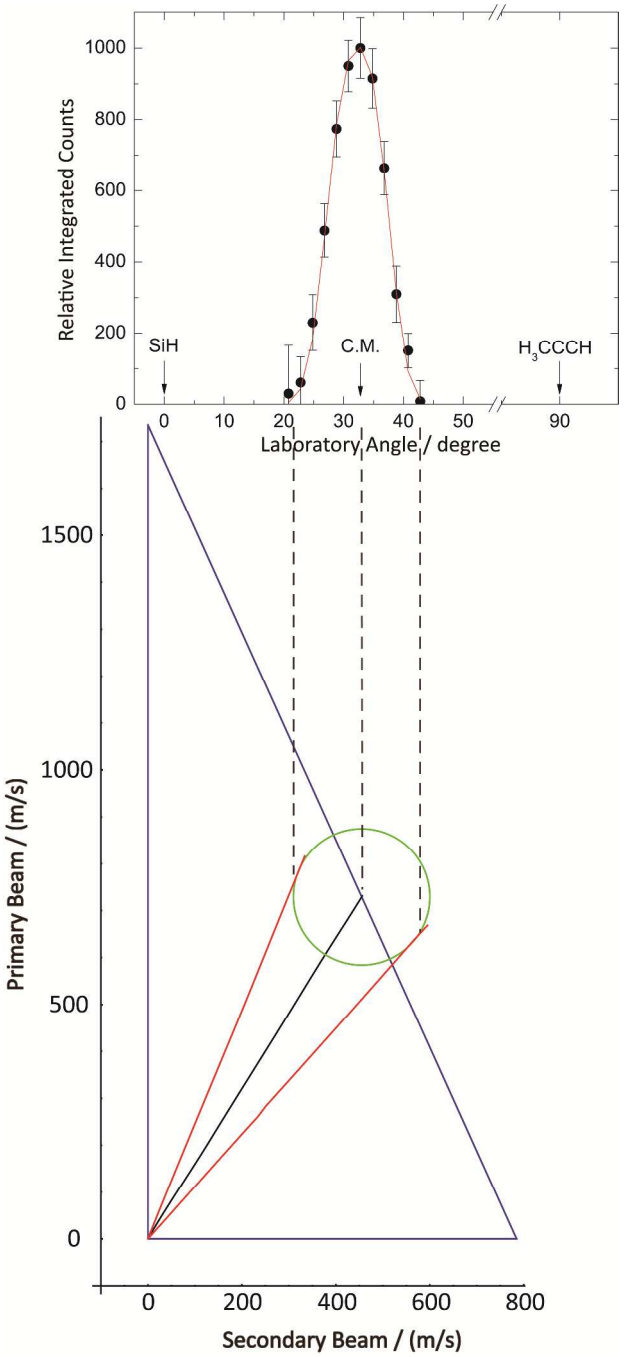


Figure 4. Laboratory angular distribution obtained at a mass-to-charge ratio (*m/z*) of 68 ($SiC_3H_4^+$) in the reaction of the silylidyne radical (SiH; $X^2\Pi$) with methylacetylene ($CH_3CCH$; $X^1A_1$) (top) along with the most probable Newton diagram leading to $SiC_3H_4$ isomer(s) (bottom). The Newton circle represents the maximum center-of-mass recoil velocity of the thermodynamically most stable 2-methyl-1-silacycloprop-2-enylidene ($SiC_3H_4$) isomer.

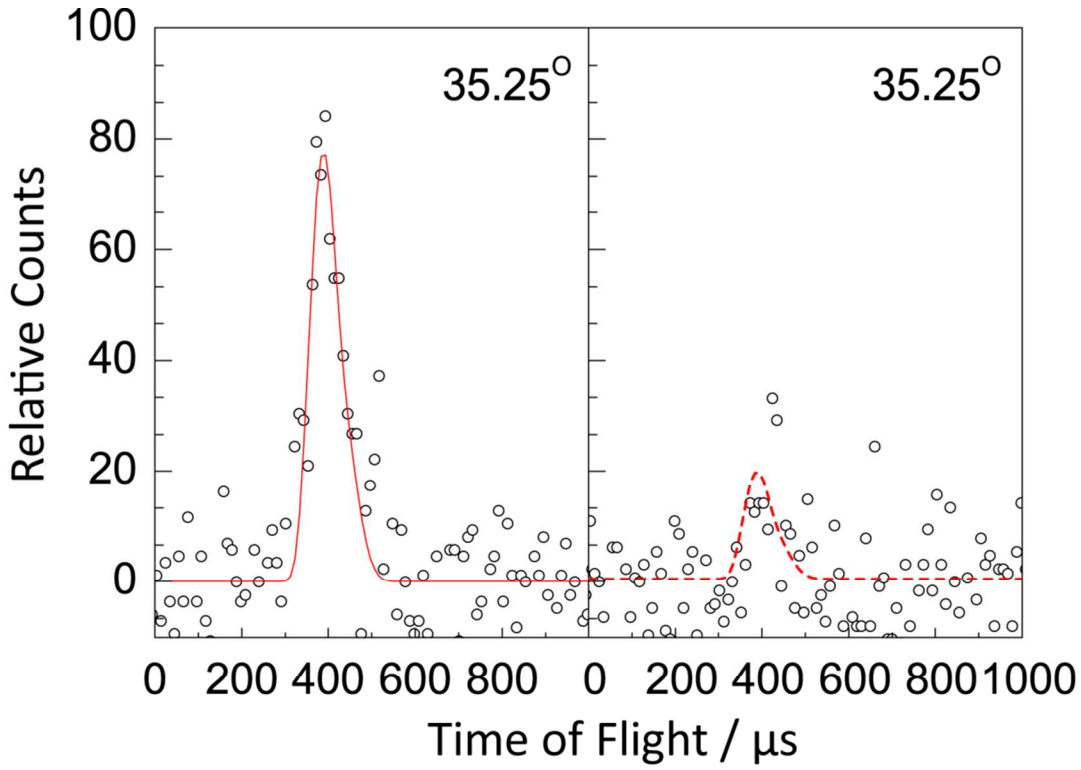


Figure 5. The center-of-mass TOF spectra for the reaction of the silylidyne radical (SiH; $X^2\Pi$) with D4-methylacetylene ($CD_3CCD$; $X^1A_1$) recorded at *m/z* = 72 ($SiC_3D_4^+$) for the atomic hydrogen loss channel (left). Signal at *m/z* = 71 (right) is – if any - barely recognizable; the dashed line represents the best fit simulation for the dissociative electron impact fragmentation of $^{29}SiC_3D_4^+$ (*m/z* = 73) to $^{29}SiC_3D_3^+$ (*m/z* = 71); the circles represent the experimental data.

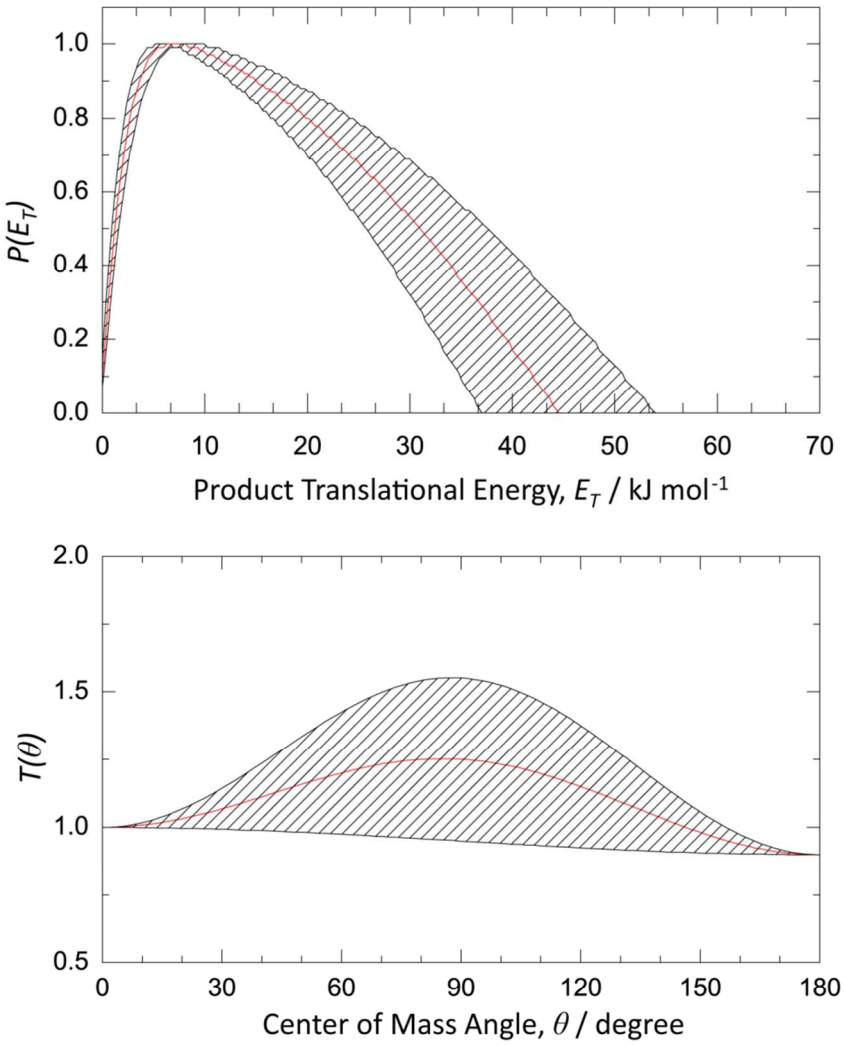


Figure 6. Center-of-mass translational energy distribution *P(E$_T$)* (top) and angular distribution *T(θ)* (bottom) for the reaction of the silylidyne radical with methylacetylene forming $SiC_3H_4$ product isomer(s) via an atomic hydrogen emission. The hatched areas define the error limits.

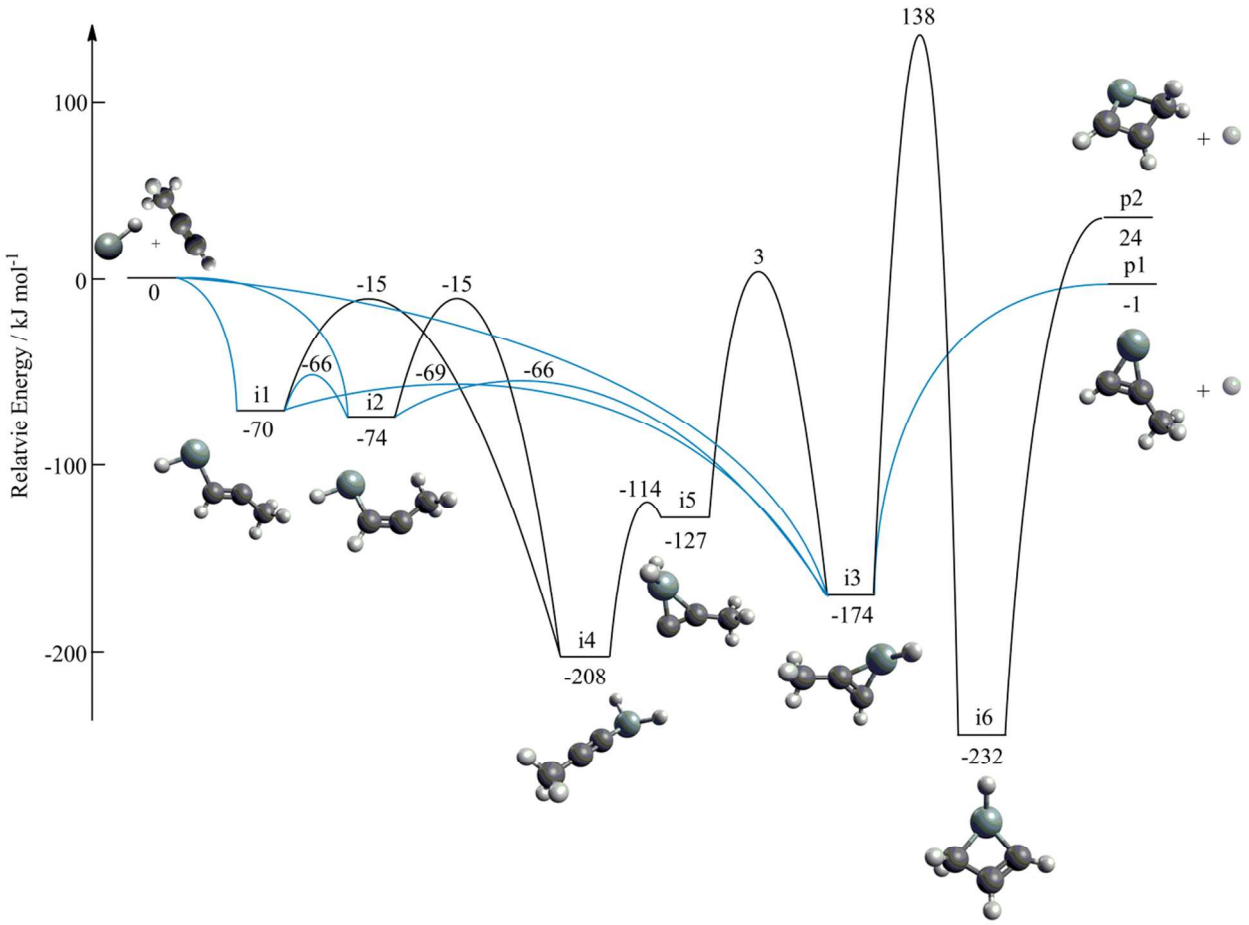


Figure 7. Relevant stationary points of the $SiC_3H_5$ potential energy surface for the reaction of the silylidyne radical (SiH; $X^2\Pi$) with methylacetylene ($CH_3CCH$; $X^1A_1$). Energies of the intermediates, transition states, and products are given relative to the reactants energy in kJ $mol^{-1}$. The elucidated reaction pathway [i1]/[i2]([i3]) →[i3] →**p1**+H is highlighted in blue.

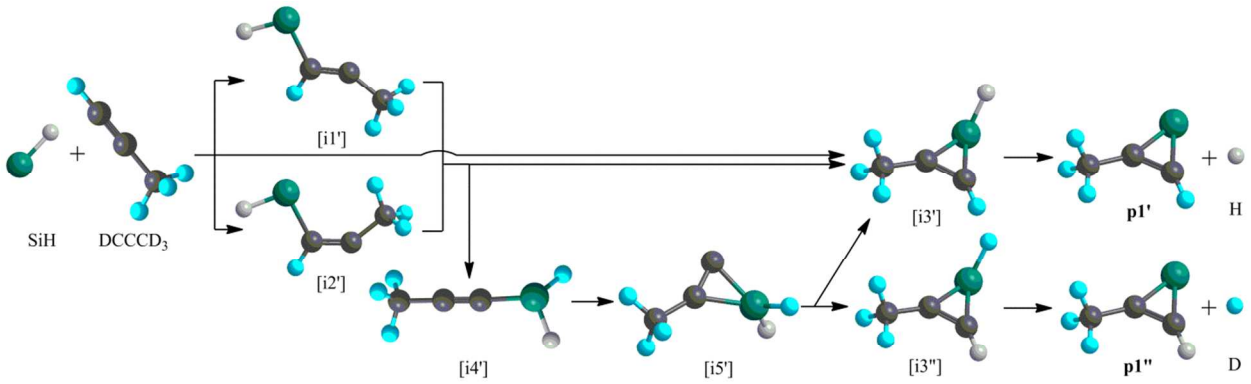


Figure 8. Reaction pathways leading from the silylidyne radical with D4-methylacetylene to the most preferential route [i1']/[i2'](**[i3']**)→ [i3'] → **p1'**+H, comparing with the inaccessible reaction route [i1']/[i2']→[i4']→[i5']→[i3']/[i3"] → **p1'**+H/**p1"**+D, under current experimental conditions.

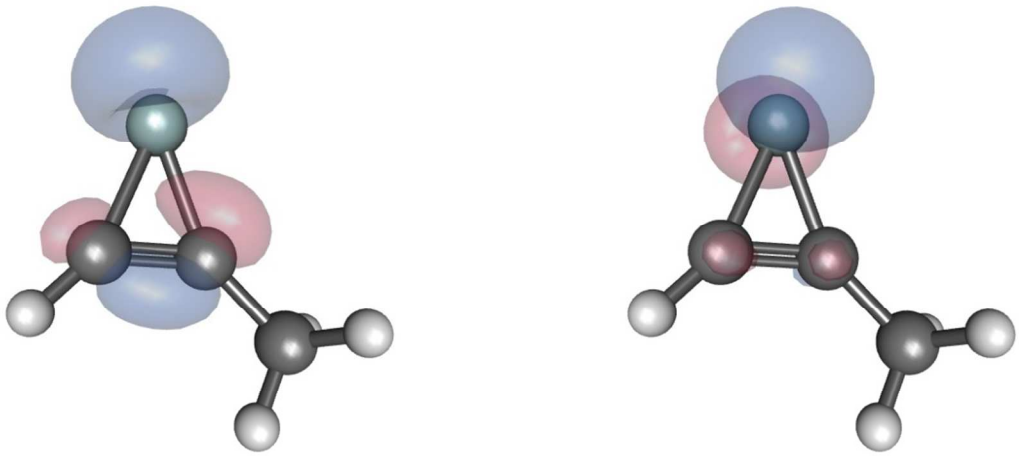

Figure 9. Schematic representation of the HOMO (left) and LUMO (right) of the 2-methyl-1-silacycloprop-2-enylidene product.

TOC

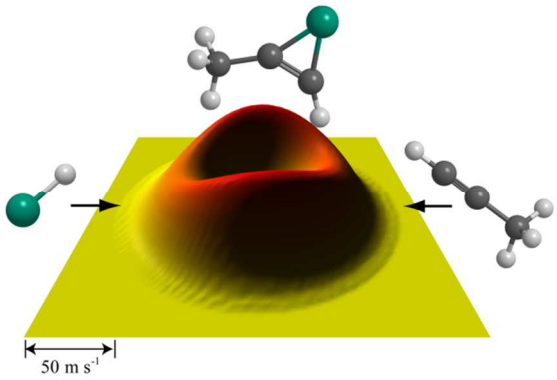


Graphical Abstract: Flux contour map for the crossed beam reaction of the silylidyne radical (SiH; $X^2\Pi$) with methylacetylene ($CH_3CCH$; $X^1A_1$) leading via atomic hydrogen loss to the 2-methyl-1-silacycloprop-2-enylidene ($SiC_3H_4$) product.